Hoxb3 negatively regulates *Hoxb1* expression in mouse hindbrain patterning

Elaine Y. M. Wong[1], Xing An Wang[1], Siu Shan Mak[1], Jearn Jang Sae-Pang[1], Kam Wing Ling[1], Bernd Fritzsch[2] and Mai Har Sham[1,*]

[1]Department of Biochemistry and Centre for Reproduction, Development and Growth, Li Ka Shing Faculty of Medicine, The University of Hong Kong, Pokfulam, Hong Kong SAR, China; and [2]Department of Biology, The University of Iowa, USA.

Short running title: Hoxb3 suppresses *Hoxb1* expression directly

Keywords: *Hoxb3, Hoxb1*, rhombomere 4, hindbrain patterning, facial branchiomotor neurons, neurogenesis, Hox gene regulation, neuronal identity, posterior prevalence

*Correspondence should be addressed to:
Dr. Mai Har Sham, Department of Biochemistry, The University of Hong Kong, Faculty of Medicine Building, 21 Sassoon Road, Pokfulam, Hong Kong SAR, China.
Tel: (852) 28199195; Fax: (852) 28551254; E-mail: mhsham@hkucc.hku.hk.

Abstract

The spatial regulation of combinatorial expression of *Hox* genes is critical for determining hindbrain rhombomere (r) identities. To address the cross-regulatory relationship between *Hox* genes in hindbrain neuronal specification, we have generated a gain-of-function transgenic mouse mutant *Hoxb3*^{Tg} using the *Hoxb2* r4-specific enhancer element. Interestingly, in r4 of the *Hoxb3*^{Tg} mutant where *Hoxb3* was ectopically expressed, the expression of *Hoxb1* was specifically abolished. The hindbrain neuronal defects of the *Hoxb3*^{Tg} mutant mice were similar to those of *Hoxb1*$^{-/-}$ mutants. Therefore, we hypothesized that *Hoxb3* could directly suppress *Hoxb1* expression. We first identified a novel Hoxb3 binding site S3 on the *Hoxb1* locus and confirmed protein binding to this site by EMSA, and by in vivo ChIP analysis using P19 cells and hindbrain tissues from the *Hoxb3*^{Tg} mutant. We further showed that *Hoxb3* could suppress *Hoxb1* transcriptional activity by chick in ovo luciferase reporter assay. Moreover, in E10.5 wildtype caudal hindbrain, where *Hoxb1* is not expressed, we showed by in vivo ChIP that Hoxb3 was consistently bound to the S3 site on the *Hoxb1* gene. This study reveals a novel negative regulatory mechanism by which *Hoxb3* as a posterior gene serves to restrict *Hoxb1* expression in r4 by direct transcriptional repression to maintain the rhombomere identity.

Introduction

The mammalian hindbrain functions to control motor activity, sensory perception, balance and coordination. The complex neuronal circuits that connect neurons to their targets depend on the generation of distinct neuronal populations in a precise spatial order along the anteroposterior and dorsoventral axes in the developing hindbrain. During embryogenesis, the hindbrain undergoes transient segmentation into seven rhombomeres. Each rhombomere has a unique identity that defines the generation of specific types of branchial, somatic and visceral motor neurons. The combinatorial expression pattern of *Hox* genes forms the branchial 'Hox code' that confers the axial identity of the hindbrain rhombomeres, specifies the generation of appropriate sensory and motor neurons and coordinates the innervation of tissues in the branchial region (Briscoe and Wilkinson, 2004; Fraser et al., 1990; Keynes and Krumlauf, 1994; Kulesa and Fraser, 1998; Kulesa and Fraser, 2000; Lumsden and Krumlauf, 1996).

A characteristic feature of mammalian *Hox* genes is the temporal and spatial colinear relationship between their organization within gene clusters and their ordered overlapping expression patterns along the anterior-posterior axis during development. The spatiotemporal expression patterns of *Hox* genes in the hindbrain are subjected to a complex network of transcriptional and post-transcriptional regulations. There are also auto- and cross-regulations among *Hox* genes that contribute to the establishment and maintenance of their dynamic expression patterns during hindbrain development (Maconochie et al., 1996; Tumpel et al., 2009). By genetic mutation studies in mice, a number of *Hox* genes have been demonstrated to function as positive regulators to control

Hox expression. The negative cross-regulatory mechanism that is essential for restricting the expression and function of *Hox* genes to specific anteroposterior domains, which leads to the posterior prevalence of *HOM-C* genes in *Drosophila* (Duboule and Morata, 1994; Morata, 1993), is not well described among mammalian *Hox* genes.

In the developing mouse neural tube, the earlier expressing genes are initiated from posterior and their expression domains extend to anterior. Later, their anterior expression boundaries are established and coincide with the hindbrain rhombomere boundaries. The posterior boundaries of expression of *Hox* genes in the neural tube are not well defined, with the exception of *Hoxb1* which is initially expressed broadly in the neural tube, but restricted to r4 by E9.0. The initiation of *Hoxb1* expression is achieved by retinoid signaling (Huang et al., 2002; Marshall et al., 1994), positive auto-regulation by *Hoxb1* further maintains its expression in r4 (Ferretti et al., 2005; Gavalas et al., 2003; Popperl et al., 1995; Studer et al., 1998). Retinoic acid can also act as a negative regulator to repress *Hoxb1* expression in r3/r5 from E9.5 and at later stages (Studer et al., 1994). Nevertheless, these negative regulatory mechanisms have been shown to be insufficient in restricting the expression of *Hoxb1* to r4. In a transgenic experiment in defining the genomic sequence requirement, additional negative regulatory mechanisms have been implicated in the repression of *Hoxb1* expression (Fox, 2000). Therefore, how *Hoxb1* expression is restricted specifically within the r4 boundary is still not fully understood. The *Hoxb3* gene is expressed in the posterior neural tube and extended to r5, with an anterior boundary at r4/5 and this expression domain is complementary to the expression territory of *Hoxb1*. Based on the evolutionary conserved posterior prevalence model, *Hoxb3* could

be a candidate negative regulator of *Hoxb1* and suppress the expression of *Hoxb1* in the neural tube caudal to r4. However, the molecular mechanism for the posterior gene *Hoxb3* to repress the anterior gene *Hoxb1* is unknown.

By genetic analysis using gain- or loss-of-function mutations and examining neuronal abnormalities of mutant embryos, it has been shown that *Hox* genes are required in early rhombomere patterning and subsequent specification of neuronal cell fates. In particular, the *Hox1* and *Hox3* genes are required for normal rhombomere (r) 4 and r5 neuronal specification. Targeted inactivation of *Hoxa1* leads to reduction of r4 and absence of r5, loss of r5 lateral motor nuclei that send efferent fibers to the VIIth nerve, and altered expression of *Math3, Phox2b, Gata2* in r4 with many associated neuronal defects (Carpenter et al., 1993; Gavalas et al., 2003). Disruption of *Hoxb1* leads to a failure to specify facial brachiomotor neurons (FBM) and contralateral vestibuloacoustic (CVA) efferent neurons within r4, and migration of FBMs to r5 and r6 is also defective (Goddard et al., 1996; Studer et al., 1996). The phenotype of *Hoxb2* knockout mutants is similar to those of *Hoxb1* knockout mutants but less severe (Gavalas et al., 2003); *Hoxb2* inactivation leads to reduced *Math3, Gata2* and *Phox2b* expression in r4, and reduced migration of r4 FBMs to r5. While individual *Hox3* mutants did not have evident hindbrain defects, in *Hoxa3* and *Hoxb3* double knockout mutants, the somatic motoneurons (SMNs) in r5 are completely absent at E11.5, *Olig2* expression which marks SMN progenitors are absent and the region normally occupied by SMNs are instead occupied by V2 neurons (Gaufo et al., 2003). Over-expression of *Hoxa3* in chick

anterior hindbrain could also lead to generation of ectopic SMNs, suggesting that *Hoxa3* can specify somatic motor neuron cell fate (Guidato et al., 2003).

In order to address the cross-regulatory relationship between *Hoxb1* and *Hoxb3*, and to investigate the effect of altering the combinatorial *Hox* code on hindbrain patterning and neuronal specification, we have generated a gain-of-function $Hoxb3^{Tg}$ transgenic mutant using the *Hoxb2* r4-specific enhancer element (Ferretti et al., 2000; Maconochie et al., 1997) to ectopically express *Hoxb3* in r4. Interestingly, we found that the $Hoxb3^{Tg}$ mutant mice displayed a loss of *Hoxb1* expression in r4, and the hindbrain neurogenesis defects were similar to the $Hoxb1^{-/-}$ mutant phenotypes (Gaufo et al., 2000; Gavalas et al., 2003; Goddard et al., 1996; Studer et al., 1996). To further investigate whether *Hoxb3* could directly repress *Hoxb1* expression, we have identified a novel Hoxb3 binding site on the *Hoxb1* locus by bioinformatics analysis. Moreover, by in vitro and in vivo molecular analysis we have obtained molecular evidence that Hoxb3 directly binds to *Hoxb1* through the Hoxb3 binding site and negatively regulate *Hoxb1* transcription. Here we demonstrate a novel negative regulatory mechanism by which *Hoxb3* as a posterior gene serves to restrict *Hoxb1* expression in r4 by direct transcriptional repression to maintain the rhombomere identity in order to specify distinct neuronal subtypes.

Materials and Methods

Generation of *Hoxb3* gain-of-function transgenic mutants

The transgenic construct was generated by cloning the 1.4 kb *Hoxb2* r4 and 2nd BA specific enhancer element (Ferretti et al., 2000; Maconochie et al., 1997; Manzanares et al., 1999), *β-globin* promoter fragment, 2.6 kb *Hoxb3* genomic DNA and SV40 3' untranslated and polyadenylation region into the pPolyIII vector. For the *Hoxb3* genomic DNA, the 5' fragment of ~200 bp from the ATG start codon to the *Sac*I site was amplified by PCR using the primer pairs 5'-TCTAG AGCAT GCAGA AAGCC ACCTA-3' and 5'-TGCAG CTGCC ATTGA GCTCC-3'. The 3' fragment was a 2.4 kb *Sac*I-*Hind*III genomic DNA of *Hoxb3* containing a *myc*-tag at the *Bam*HI site (Sham et al., 1992). The DNA transgene was released from the vector by *Xho*I digestion and the 5.4 kb transgenic fragment was isolated and purified for oocyte microinjection. For the generation of transgenic founders, fertilized oocytes from superovulated FVB mice were used. Three independent transgenic mouse lines, designated $Hoxb3^{Tg2}$, $Hoxb3^{Tg7}$ and $Hoxb3^{Tg8}$, were maintained in FVB genetic background.

Mouse genotyping

For genotyping of *Hoxb3* mutants by PCR amplification, the primers used were 5'-CCACT AGGCC TAGAC TAGC-3' derived from the *Hoxb2* r4 enhancer and 5'-TGCAG CTGCC ATTGA GCTCC-3' derived from exon 3 of *Hoxb3* (arrows in Fig. 1A). Genomic DNA was digested with *Sac*I, the *Bgl*II-*Eco*RI fragment from the *Hoxb2*

r4 enhancer and *Bam*HI-*Hind*III fragment from the *Hoxb3* gene were used as 5' and 3' probes in Southern hybridization.

RNA *in situ* hybridization

Whole-mount *in situ* hybridization was performed using DIG-labeled riboprobes and visualized by NBT/BCIP (Roche) (Wilkinson et al., 1992).

Neuronal tract tracing

Facial branchial motoneurons (FBMs) and contralateral vestibuloacoustic (CVA) neurons of E11.5 mouse embryos were labeled using NeuroVue® dye-coated filters (MTTI) (Fritzsch and Nichols, 1993). Selective tracing was achieved by inserting the red dye filter into the inner ear for efferent neurons and inserting the green dye filter into the facial nerve for facial branchial and visceral motoneurons. Labeled brain samples were dissected and flat-mounted in glycerol. Fluorescent images were obtained using a Leica LAS AF confocal microscope.

Bioinformatics analysis of Hoxb3 binding site

Hoxb3 consensus binding site TCATTAATTGGC (core binding sequence underlined) was defined by comparative genomic analysis (Sham et al, unpublished). To identify potential Hoxb3 binding sites in the *Hoxb1* locus, the conserved regions among the *Hoxb1* and flanking sequences from six vertebrate species were found in UCSC Genome database.

Electrophoretic Mobility Shift Assay (EMSA)

Oligonucleotides, S3-WT, 5'-TCACT GCTTT TCTTC ATTTA ATTGA AATTG CCATC AAGCT TGG-3'; S3-M1, 5'-TCACT GCTTT TCCCG GCCTA ATTGA AATTG CCATC AAGCT TGG-3'; S3-M2, 5'-TCACT GCTTT TCTTC ATCCG GCCCA AATTG CCATC AAGCT TGG-3'; S3-M12, 5'-TCACT GCTTT TCCCG GCCCC GGCCA AATTG CCATC AAGCT TGG-3', designed with 5'-overhangs after annealing with their complementary strands, were labeled with [α-^{32}P]dCTP (PB10205; Amersham) by end-filling 5'-overhangs using Klenow fragment. GST-Hoxb3 fusion protein and DNA-protein binding reactions were set up as previously described (Yau et al., 2002). A 20 μl binding reaction contained 40,000 cpm oligonucleotide probe, 500 ng poly(dIdC-dIdC), protein (GST-Hoxb3, 0.2–1.6 μg), 20 mM Hepes–KOH (pH 7.9), 100 mM KCl, 0.25 μg/μl BSA, 2 mM DTT, 1 mM EDTA, 12% glycerol. The binding reaction was incubated at 24°C for 30 min. The samples were separated in a 4% acrylamide glycerol gel.

P19 Cell Culture

P19 cells were cultured on gelatin-coated (0.1%) tissue culture dishes in DMEM medium (Gibco) supplemented with 10% FBS. On day 0, cells were detached and cultured in bacterial culture dish at a density of $5x10^4$ cells/ml with DMEM medium supplemented with 10% FBS. On day 1, 10^{-8}M RA was added to the medium. The medium was refreshed with the same concentration of RA on day 3, and the P19 cells were harvested for ChIP assay on day 4.

Chromatin immunoprecipitation (ChIP) assay

ChIP assay (Hu and Rosenblum, 2005) was performed with the following modifications. For RA-treated P19 cells, $1x10^6$ cells were harvested for each assay. For *in vivo* ChIP, the forebrain, spinal cord and the ectopic sites r4/2^{nd} BA of 4 litters of E9.5 wildtype or mutant embryos were dissected in PBS. The cells or fresh tissues were fixed in 1% formaldehyde for 20 minutes at 25°C, and then disintegrated with RIPA buffer. The cross-linked material was sonicated to 200-1000 bp fragments (Vibracell sonicator; seven times for 10 seconds at 40% output), 2-4 µg of Hoxb1 (Santa Cruz, H170, sc-28603) or Hoxb3 antibody (Santa Cruz, C20, sc-17169) or normal rabbit IgG were then used to pull down the chromatin. PCR amplifications were performed using the following primers: for S1: forward: 5'-ACGTA GGTGG TGACT TGGAA CT-3', reverse: 5'-AGAGA TGGCC TATGT GCTGT GA-3'; for S3: forward: 5'-TGGGG TGCAG CGATG AGGAA-3', reverse: 5'-GCCCT AACCA CTGTC CCGCC CT-3'; for B3ARE: forward: 5'-TGGAA ACTGG TAGGT GTGTG GGC-3', reverse: 5'-TGTAT GAAGG TGAAG GAGCA GA-3'; for B1ARE: forward: 5'-TCCCT CTGGT CCCTT CTTTC-3', reverse: 5'-GAGCT GAGCA GGGGG GAAAA-3'.

Chick *in ovo* electroporation and luciferase activity assay

pCIG-Hoxb3 cDNA construct or *pCIG* empty expression vector as control was electroporated into the hindbrain r3-5 regions of Hamburger and Hamilton (HH) stage 11 to 12 chick embryos along with a firefly luciferase reporter construct containing a 600 bp fragment including the Hoxb3 binding site S3 and the RARE 3'DR2 element of the *Hoxb1* loci (Hoxb1-luc), or with the mutation of Hoxb3-binding site S3 (*mHoxb1*-luc

constructs), or pGL3 luciferase vector as control, and the CMV-*Renilla* luciferase plasmid for normalization (Promega). After 24 hours, embryos were processed for the luciferase assay as previously described (Dessaud et al., 2007). Briefly, embryos were homogenized in passive lysis buffer on ice and firefly and *Renilla* luciferase activities were measured with the Dual Luciferase Reporter Assay System (Promega).

Results

Hoxb3 is ectopically expressed in r4 of Hoxb3^{Tg} transgenic mutant

Using the transgenic construct with *Hoxb2* r4-specific enhancer and *Hoxb3* coding sequence (Fig.1A), 8 transgenic founders (designated *Hoxb3^{Tg1}* to *Hoxb3^{Tg8}*) were generated. Among the 8 founders, only *Hoxb3^{Tg2}*, *Hoxb3^{Tg7}* and *Hoxb3^{Tg8}* were fertile and 3 independent transgenic mouse lines were subsequently established. The *Hoxb3^{Tg}* mutants were genotyped by PCR (Fig. 1A); by Southern blotting analysis, the *Hoxb3^{Tg2}*, *Hoxb3^{Tg7}* and *Hoxb3^{Tg8}* transgenic mutant lines were estimated to contain approximately 12, 2 and 6 copies of transgenic DNA respectively (Fig. 1B). By Western blotting, ectopic Hoxb3 protein could be detected in rhombomere 4 and the second branchial arch in E10.5 *Hoxb3^{Tg}* mutant embryos obtained from the three different mouse lines (Fig. 1C). Wildtype, heterozygous (*Hoxb3$^{Tg/+}$*) and homozygous (*Hoxb3$^{Tg/Tg}$*) mice were born in expected Mendelian ratio. All three *Hoxb3^{Tg2}*, *Hoxb3^{Tg7}* and *Hoxb3^{Tg8}* transgenic mouse lines displayed similar phenotypes of craniofacial dysmorphology (Suppl. Fig. 1 and Table 1). *Hoxb3$^{Tg/+}$* mutants appeared smaller in size (data not shown) and *Hoxb3$^{Tg/Tg}$* mutants died shortly after birth, possibly due to feeding disability rather than a direct effect of the transgene. We focused our analysis on the *Hoxb3^{Tg2}* line which has the highest number of copies of the transgene.

In *Hoxb3$^{Tg/+}$* embryos, ectopic *Hoxb3* expression could be detected in the anterior neural tube as early as E7.5 and E8.5 (Fig. 3E, F). At E9.0, ectopic *Hoxb3* was expressed in r4 of the neural tube, the entire developing otic cup, 1st and 2nd BAs (Fig. 1D). At E9.5,

ectopic expression of *Hoxb3* was maintained in the hindbrain at r4 (Fig. 3G), 2nd BA, the proximal surface ectoderm of the 1st BA and dorsal region of the otic vesicle (Fig. 1D). Interestingly, endogenous expression of *Hoxb3* in r5 was also maintained at a high level in the mutant when compared with wildtype at E10.5 (Fig. 1D and Fig. 3H). The posterior expression of *Hoxb3* in the neural tube was not affected in *Hoxb3*$^{Tg/+}$ embryos.

Hoxb3$^{Tg/+}$ *mutants have facial nerve abnormalities*

Compared to wildtype (Fig. 2A-C and Suppl. Fig. 1A,B), 6 out of 8 transgenic founder mice showed similar overt phenotypes including narrower face (Fig. 2E and Suppl. Fig. 1D,G,J); receded lower lip, impaired whisker movement and facial paralysis (Fig. 2F and Suppl. Fig. 1E,H,K); abnormal preyer reflex, abnormal reaching response (Fig. 2G), head tilting and circling behaviour (data not shown). Wildtype and *Hoxb3*$^{Tg2/+}$ mutant adults were sacrificed and facial somatic motor components of the VIIth cranial nerve were exposed for analysis. In wildtype (Fig. 2D and Suppl. Fig. 1C), the zygomatic, buccal and the mandibular branches of the facial nerve were readily recognizable. However, in mutant adults from *Hoxb3*$^{Tg2/+}$ (Fig. 2H) and other transgenic lines (Suppl. Fig. 1F,I,L), the mandibular branch of the facial nerve was either reduced or absent which resembled that of the *Hoxb1* knockout mice reported previously (Goddard et al., 1996; Rossel and Capecchi, 1999; Studer et al., 1998; Studer et al., 1996).

Hindbrain segmentation in Hoxb3$^{Tg/+}$ *mutants*

As *Hoxb3* was ectopically expressed in the hindbrain at more anterior regions, and specifically in r4 from E9.0 onwards, we examined whether there were hindbrain

segmentation defects in *Hoxb3*^{Tg} mutants using several rhombomere-specific markers. At E8.5, *Wnt8a* was expressed in r4 of wildtype embryos (4-7 somite stage) (Fig. 3S) (Bouillet et al., 1996). Interestingly, in *Hoxb3*$^{Tg/+}$ embryos of similar somite stages, expression of *Wnt8a* could not be detected in the mutant r4 (Fig. 3U), suggesting that the identity of r4 was lost in the *Hoxb3*^{Tg} mutant. Expression of the r3 and r5 marker genes *Krox20* (Fig. 3Y) and *EphA4* (Fig.3Z) in *Hoxb3*$^{Tg/+}$ mutants at E8.5 and E9.5 were the same as in wildtype littermates (Fig. 3W,X). *Kr* expression in r5 and r6 in *Hoxb3*$^{Tg/+}$ mutants (Fig. 3V) examined at E9.5 was also the same as in wildtype (Fig. 3T). The *Wnt 8a, Krox20, EphA4* and *Kr* expression profiles in *Hoxb3*$^{Tg/+}$ mutants indicate that enforced expression of *Hoxb3* in r4 did not affect the establishment of the r4 territory nor hindbrain segmentation, but changed the identity and properties of r4.

Hoxb1 is down-regulated by ectopic Hoxb3 expression in r4

In wildtype embryos (Fig. 3I), *Hoxb1* expression was activated at E7.5, and subsequently restricted to r4 and the posterior mesoderm at E8.5-10.5 (Fig. 3J-L). In *Hoxb3*$^{Tg/+}$ embryos (Fig. 3N), *Hoxb1* expression was found to reach the anterior boundary at E7.5 as in wildtype embryos. Interestingly, no expression of *Hoxb1* could be detected in the hindbrain region at E8.5 (Fig. 3O), E9.5 (Fig. 3P) or E10.5 (Fig. 3Q), though expression in the pre-somitic mesoderm could still be readily observed. Therefore, *Hoxb1* expression in *Hoxb3*$^{Tg/+}$ transgenic embryos was specifically abolished in r4 (Fig. 3O-Q) but was maintained in the posterior (Fig. 3O). Enforced expression of *Hoxb3* in the anterior neural domains at E8.5 (arrowhead in Fig. 3F) suppressed the expression of *Hoxb1* specifically in r4, and this suppression was maintained through later stages of

development (Fig. 3O-Q). The suppression of *Hoxb1* expression in r4 was observed in all three mutants lines *Hoxb3*^{Tg2}, *Hoxb3*^{Tg7} and *Hoxb3*^{Tg8} (Suppl. Fig. 1M). Consistent with the suppression of *Hoxb1*, the expression of *Hoxb2* which is a downstream target of *Hoxb1*, was specifically down-regulated in r4 where ectopic *Hoxb3* was expressed in the *Hoxb3*$^{Tg/+}$ embryos (asterisk in Fig. 3R and Suppl. Fig. 2C,D). The expression of *Hoxa2* was not affected (Suppl. Fig. 2G,H).

Abnormal neurogenesis in r4 of Hoxb3$^{Tg/+}$ *mutants*

We next addressed the impact of an altered *Hox* code on the identity of r4 by examining the characteristic neurogenesis patterns in the hindbrain of the *Hoxb3*$^{Tg/+}$ mutants. In E11.5 wildtype embryos, facial branchial motoneurons (FBMs) expressing *Islet1*, *Phox2b* and *Tbx20* were generated in the ventral domain of r4 and started to migrate through r5 to r6 (Fig. 4A-C), However, in *Hoxb3*$^{Tg/+}$ mutant embryos, the distinctive expression patterns of *Islet1*, *Phox2b* and *Tbx20* in the ventral hindbrain at r4, r5 and r6 could no longer be observed (Fig. 4F-H). In wildtype hindbrain, *Gata3* was expressed in the ventral region of r4 at E11.5 which is the downstream effector of *Hoxb1* (Pata et al., 1999) (Fig. 4D), but in r4 of *Hoxb3*$^{Tg/+}$ embryos the expression of *Gata3* was specifically down-regulated (Fig. 4I). Consistent with the changes in gene expression patterns, we confirmed by retrograde dye-tracing experiments that the facial brachial motor nucleus was absent in r6 and no migration of FBMs through r5-6 could be detected (Fig. 4M), and the number of contralateral vestibuloacoustic (CVA) neurons migrating across the midline was significantly reduced (Fig. 4N) in r4 of E11.5 *Hoxb3*$^{Tg/+}$ mutants. From these analyses, the identity of r4 was clearly lost in the *Hoxb3*$^{Tg/+}$ mutant. As a consequence of

loss of *Hoxb1* expression in r4, FBMs were not specified and the migration of motor neurons and CVA neurons impaired.

To investigate whether the abnormal r4 phenotype in the *Hoxb3*$^{Tg/+}$ mutant is due to loss-of-function of *Hoxb1* alone, or also due to gain-of-function of *Hoxb3* which might impose an r5-like identity, we compared the neurogenesis pattern of r4 with that of r2, r5 and r6 in wildtype and *Hoxb3*$^{Tg/+}$ mutants at E11.5. Firstly, in wildtype E11.5 embryos, Islet1-positive trigeminal motor nucleus had migrated from ventral to the dorsal region of r2 (Fig. 4O) and Islet1-positive FBMs were found in ventral r4-r6 (Fig. 4O). However, in r4 of *Hoxb3*$^{Tg/+}$ mutants, the cluster of FBMs could not be detected, but a few Islet1-positive motor neurons were scattered from the ventral to the dorsal region (asterisk in Fig. 4P). The distribution of Islet1-positive motor neurons in r4 was similar to that in r2 of both wildtype and *Hoxb3*$^{Tg/+}$ mutant embryos (Fig. 4O,P). Secondly, we found that *Gata2*, which normally marks serotonergic neurons and is absent in r4 (Fig. 4E), was ectopically expressed in r4 in *Hoxb3*$^{Tg/+}$ mutants (Fig. 4J). By immunostaining of hindbrain sections, we showed that 5HT-positive serotonergic neurons were present in r2 and r5, but not in r4 of wildtype E11.5 embryos (Fig. 4Q). However, ectopic 5HT-positive serotonergic neurons were clearly present next to the floor plate in r4 of *Hoxb3*$^{Tg/+}$ mutant embryos (Fig. 4R). Thirdly, we examined the distribution of Lim3-positive interneurons in ventral r4 (Fig. 4S) and found that the location of Lim3-positive V2 interneurons were shifted to more ventral region in r4 of *Hoxb3*$^{Tg/+}$ mutants (Fig. 4T). The depletion of islet1-positive neurons, presence of ectopic 5HT-positive serotonergic neurons, and the ventral shift of p2 and p3 progenitor domains

(summarized in Fig. 4) in r4 of the *Hoxb3*$^{Tg/+}$ mutants are similar to the reported phenotype of *Hoxb1*$^{-/-}$ mutant mice (Gaufo et al., 2000; Gavalas et al., 2003; Goddard et al., 1996; Jacob et al., 2007; Pattyn et al., 2003; Studer et al., 1996).

We further examined the expression of *Islet2* which marks somatic motor neurons and found that no ectopic *Islet2* expression could be detected in r4 of *Hoxb3*$^{Tg/+}$ mutants (data not shown). Therefore, ectopic *Hoxb3* expression in r4 was insufficient to induce somatic motor neuron differentiation, the characteristic neuronal subtype for r5 could not be found in the ectopic site of the mutant. Hence the identity of r4 was changed to an r2-like rhombomere but not r5. As the neurogenesis pattern of r4 in the *Hoxb3*$^{Tg/+}$ mutant is highly similar to that of *Hoxb1*$^{-/-}$ mutant (Studer et al., 1998), the change of r4 identity in *Hoxb3*$^{Tg/+}$ mutants is likely caused by the absence of *Hoxb1* but not the presence of ectopic *Hoxb3*. Taken together, the *Hoxb3*$^{Tg/+}$ mutant is a phenocopy of the *Hoxb1*$^{-/-}$ null mutant.

Hoxb3 negatively regulates Hoxb1 by direct binding to specific genomic site

Since expression of *Hox* genes are subjected to cross-regulation, we explored the possibility that Hoxb3 may regulate *Hoxb1* expression directly by specific binding to cis-acting sequence elements. We have previously defined a Hoxb3 consensus binding site TCATTAATTGGC by comparative genomic analysis (Sham et al. unpublished). To identify potential Hoxb3 binding sites in the *Hoxb1* locus, we searched within the *Hoxb1* genomic sequences from conserved regions among six vertebrate species. Within the conserved regions, three potential Hoxb3 binding sties, S1, S2 and S3, with sequence

similarity to the Hoxb3 consensus binding site could be identified (Fig. 5A,B). The S1 and S3 sites are located in the 5' and 3' flanking regions of *Hoxb1* respectively, both of them have a TAAT core motif found in the consensus binding sequence of Hoxb3. The S2 site is located 170 bp downstream of the *Hoxb1* auto-regulatory element B1ARE and has two adjacent core motifs.

As the S3 site located 2.5 kb 3' to the *Hoxb1* coding region has an identical core sequence to our predicted Hoxb3 consensus binding site, we first tested the binding of Hoxb3 to the S3 site by *in vitro* electrophoretic mobility shift assay using bacterial expressed GST-Hoxb3 fusion protein (Yau et al., 2002). We demonstrated that GST-Hoxb3 fusion protein could bind to oligonucleotides containing the S3 site, the amount of bound oligonucleotides was proportional to the amount of GST-Hoxb3 fusion protein used (Fig. 5C, lanes 2-4). The binding of GST-Hoxb3 to the S3 site could be competed out with unlabelled wildtype S3 oligonucleotides (Fig. 5C, lanes 5-7), but not with unlabelled oligonucleotides containing mutated S3 binding sites M1, M2 and M12 (Fig. 5C, lanes 8-10). Therefore, GST-Hoxb3 fusion protein could bind specifically to the S3 site on *Hoxb1*. Similar EMSA were performed using oligonucleotides containing the S1 or S2 sites but we could not detect any specific binding of Hoxb3 to these sites (data not shown).

To test that Hoxb3 can specifically bind to the S3 binding site on *Hoxb1, in vivo* ChIP assays were performed using P19 teratocarcinoma cells and mouse embryos. Several test and control sets of primers were used to amplify chromatin fragments

immunoprecipitated with Hox antibodies in the ChIP assays, namely S1; S2/B1ARE which contains the closely linked S2 site and Hoxb1 auto-regulatory element; S3; and B3ARE which contains the Hoxb3 auto-regulatory element (Yau et al., 2002). P19 cells were treated with retinoic acid (RA) to mimic the hindbrain microenvironment (Okada et al., 2004). Our ChIP results showed that Hoxb3 antibody could precipitate the Hoxb3-B3ARE complex as expected, it also specifically pulled down the Hoxb3-S3 complex, but no binding to the S1 or S2/B1ARE sites could be detected (Fig. 6A). The pull-down of the Hoxb3-S3 chromatin complex was highly specific, as no complex formation could be detected when Hoxb4 or Hoxb1 antibodies, or IgG were used as controls in the ChIP assay. We showed that Hoxb1 antibody could pull down the S2/B1ARE complex, which was due to the presence of the closely linked Hoxb1 auto-regulatory site. Therefore, we have clearly demonstrated that in RA-treated P19 cells which expressed *Hoxb* genes endogenously, Hoxb3 protein could specifically bind to the S3 site on the *Hoxb1* gene.

To confirm that Hoxb3 could bind directly to *Hoxb1* during mouse embryogenesis, we isolated forebrain, caudal hindbrain/spinal cord and the ectopic sites r4/2nd BA tissue extracts from E9.5 wildtype and *Hoxb3*$^{Tg/+}$ mutant embryos and performed ChIP assays as above (Fig. 6B). In wildtype embryos, Hoxb3 protein could bind to the S3 site on *Hoxb1* and the B3ARE site on *Hoxb3* in the caudal hindbrain/spinal cord, indicating that Hoxb3 could directly regulate *Hoxb1*, and activate *Hoxb3* through auto-regulation in this region. No binding could be detected in the forebrain or r4/2nd BA tissues. In the *Hoxb3*$^{Tg/+}$ mutant (Fig. 6B), Hoxb3 could bind to the S3 site in the caudal

hindbrain/spinal cord as well as r4/2nd BA, indicating that Hoxb3 could directly mediate the down-regulation of *Hoxb1* via binding to the S3 site. Interestingly, in the mutant embryos, Hoxb3 could bind to the B3ARE not only in the caudal hindbrain/spinal cord region, but also in the r4/2nd BA region, suggesting that there could be Hoxb3 auto-regulation in the ectopic site which sustained the expression of *Hoxb3* in r4 of the transgenic mutant embryos. No binding could be detected in *Hoxb3*$^{-/-}$ mutant embryo samples (Manley and Capecchi, 1997), further confirming the specificity of the Hoxb3 antibody used. In summary, by in vitro EMSA and in vivo ChIP analyses, we have provided strong evidence that Hoxb3 could bind directly to the *Hoxb1* gene. Hoxb3 protein was bound to the S3 site on *Hoxb1* in r4 of the *Hoxb3*$^{Tg/+}$ mutant embryos, and in the caudal hindbrain/spinal cord of both wildtype and mutant embryos.

To assess whether Hoxb3 could negatively regulate *Hoxb1* transcription through the S3 Hoxb3 binding site in vivo, we examined the effects of overexpression of *Hoxb3* in the chick hindbrain on *Hoxb1* luciferase reporter constructs by *in ovo* electroporation experiments (Fig. 6C). Using a wildtype *Hoxb1* reporter (*Hoxb1*-luc), luciferase activity could be detected (Fig. 6C, bar 1); but in the presence of Hoxb3, the transcriptional activity of this *Hoxb1* reporter was significantly reduced (p=0.026) (Fig. 6C, bar 2). In contrast, Hoxb3 expression could not inhibit the transcriptional activity of the mutant *Hoxb1* reporter (*mHoxb1*-luc) in which the S3 binding site was mutated (Fig. 6C, bar 3). These results further demonstrate that Hoxb3 can repress *Hoxb1* transcriptional activity through the S3 Hoxb3 binding site. Together with the transgenic mouse mutant analysis which shows that in *Hoxb3*^{Tg} mutants *Hoxb1* expression in r4 is specifically suppressed,

we conclude that *Hoxb3* serves as a direct negative regulator of *Hoxb1* expression.

Discussion

Using a *Hoxb3* gain-of-function mutation approach, we have altered the combinatorial *Hox* code in the developing hindbrain rhombomere 4 of the $Hoxb3^{Tg}$ mutant mice. Through cellular and molecular analyses of the hindbrain defects of the $Hoxb3^{Tg}$ mutant, we demonstrated that *Hoxb3* could function as a direct negative regulator of *Hoxb1* gene in restricting *Hoxb1* expression to r4. As shown by in vivo embryo tissue ChIP assay (Fig. 6B), Hoxb3 binds to the *Hoxb1* gene in the caudal hindbrain, thereby represses *Hoxb1* expression during normal hindbrain development. Therefore, *Hoxb3* serves to protect the posterior hindbrain from the action of *Hoxb1*, and ensure rhombomere-specific neuronal fate determination and migration during normal hindbrain neurogenesis.

In this study we have analysed three independent transgenic mouse lines $Hoxb3^{Tg2}$, $Hoxb3^{Tg7}$ and $Hoxb3^{Tg8}$, with the cellular and molecular studies focusing on the $Hoxb3^{Tg2}$ line for consistency. Although the level of Hoxb3 protein expression varies among these mouse lines as shown by western blot analysis (Fig. 1C), all three mouse lines showed clear loss of *Hoxb1* expression in r4 (Supplementary Fig. 1M) and displayed similar craniofacial defects (Supple. Fig. 1). The lack of a gene dosage/expression level effect suggests that Hoxb3 could be a strong repressor, such that low level of *Hoxb3* expression, as seen in the $Hoxb3^{Tg7}$ line, was sufficient to suppress *Hoxb1* expression and led to distinctive abnormalities as phenocopy of *Hoxb1* null mutant. Indeed, 2 out of 8 transgenic founders had no observable phenotypes (Table 1), it is possible that in those mutant founders the expression of the *Hoxb3* transgene was below the threshold to trigger any alterations in *Hoxb1* expression. Interestingly, the *Hoxb2* r4 and BA2 enhancer used

in the *Hoxb3* transgenic construct contains Hoxb1 binding sites and its enhancer function is Hoxb1 dependent (Feretti et al 2000, Maconochie et al, 1997). In the *Hoxb3*^{Tg} mutant, when *Hoxb1* was suppressed, *Hoxb3* transgene expression could still be maintained beyond E9.5 (Fig. 1D). Clearly, other *Hoxb1*-independent mechanisms were involved in maintaining the expression of the transgene at later stages, and one possibility would be auto-regulation. In our in vivo ChIP analysis, we showed that Hoxb3 could bind to its auto-regulatory site B3ARE in the ectopic expression site of r4 and 2nd BA (Fig. 6B). Therefore, in the *Hoxb3*^{Tg} mutants, ectopic Hoxb3 expression was initially activated at around E7.5-E8.0 by *Hoxb1*; by E8.5 when *Hoxb1* expression was suppressed, the expression of *Hoxb3* could be self-sustained by an auto-regulatory mechanism through binding to the B3ARE site.

The role of Hoxb3 and Hoxb1 in hindbrain neurogenesis

By altering the *Hox* code in r4 with enforced expression of *Hoxb3*, indeed the identity of r4 in the *Hoxb3*^{Tg} mutant was changed. Most strikingly we found that the expression of *Hoxb1* in r4 was completely abolished in the mutants from E8.5. Using hindbrain rhombomere-specific markers we showed that in the *Hoxb3*^{Tg} mutant there was no apparent transformation of r4 into odd-numbered rhombomeres such as r3 or r5. Although *Hoxb3* is normally expressed and upregulated in r5 at E9.5, ectopic expression of *Hoxb3* was insufficient to impose an r5-like character in r4 of the mutant. Therefore, the hindbrain segmentation and the establishment of the r4 territory were not affected in the *Hoxb3*^{Tg} mutant, but the identity of r4 was lost with the loss of *Hoxb1* expression.

The gross phenotype of the *Hoxb3*^{Tg} mutants including narrower face, impaired whisker movement, facial paralysis, retracted lower lip and abnormal facial motor nerves are similar to that displayed in the *Hoxb1*$^{-/-}$ mutants (Arenkiel et al., 2004; Goddard et al., 1996; Studer et al., 1996). Our neuronal phenotype analysis also confirms that the *Hoxb3*^{Tg} mutant is a phenocopy of the *Hoxb1* null mutants. In r4 of the *Hoxb3*$^{Tg/+}$ mutant hindbrain, the FBMs were not specified, CVA neurons were reduced, ectopic serotonergic neurons were induced, the distributions of interneurons and efferent neurons were altered. In addition, the ectopic motor neurons in r4 of *Hoxb3*^{Tg} mutants marked by Islet1 and Tbx20 antibodies were clustered into two populations (Fig. 4F,H). One population of motor neurons formed a column in the medial-ventral region of r4, whereas a separate population of motor neurons was located in the dorsal-lateral region, at a position similar to that occupied by the trigeminal motor nucleus in r2 along the dorsoventral axis of the rhombomere. While the distribution of the Islet1-positive motor neurons in the affected r4 forms the basis for the suggestion that there is a transformation of r4 to an r2-like rhombomere, the identities of those two populations of motor neurons remain unclear and the regulation of the rhombomere-specific dorsoventral distribution of motor neurons deserves further characterization.

It has been previously shown that in r5 of the *Hoxa3*$^{-/-}$ mutants, somatic motorneurons (SMs) are reduced; and in r5 *Hoxa3*$^{-/-}$:*Hoxb3*$^{-/-}$ double mutant hindbrains, SMs are completely lost and replaced by ectopic V2 interneurons (Gaufo et al., 2003). Therefore, it is suggested that in r5, *Hoxa3* and *Hoxb3* are both required for the determination of the fate of SMs at early stages. *Hoxa3* gain-of-function study in chick embryos has

demonstrated that *Hoxa3* is sufficient to induce SMs in r1-r4 (Guidato et al., 2003). We examined the neuronal phenotypes of the $Hoxb3^{Tg}$ mutant and could not identify any r5-like SMs in r4. Therefore, in mouse embryos, *Hoxb3* alone is insufficient specify somatic motor neurons in an r4 territory. Also, even when *Hoxb3* is over-expressed in r4, it is insufficient to confer an r5-like identity in the mutant r4. Taken together, *Hoxb3* is required to interact with *Hoxa3* in order to induce the generation of SMs. Therefore, in the $Hoxb3^{Tg}$ mutant, there is a possible r4 to r2 identity switch, but not an r4 to r5 identity switch.

Hoxb3 suppresses Hoxb1 in hindbrain patterning

By both in vitro and in vivo molecular analyses, we showed that Hoxb3 can repress *Hoxb1* transcriptional activity through a specific Hoxb3 binding site located 3' to the *Hoxb1* gene, clearly demonstrating that *Hoxb3* serves as a direct negative regulator of *Hoxb1* expression. The function of *Hoxb3* as a negative regulator of *Hoxb1* could explain the regulation of *Hox* expression during normal hindbrain patterning. Within the functional domain of *Hoxb3* in the neural tube, the posterior gene *Hoxb3* represses the anterior gene *Hoxb1*, supporting the posterior prevalence model of *Hox* gene cross-regulation. As illustrated in Fig. 7A, during normal development, *Hoxb1* is expressed at E7.5 in a broad region of the neuroectoderm along the anteroposterior axis, while *Hoxb3* is expressed at a low level in the posterior neural tube. The expression pattern of *Hoxb3* then extends anteriorly and is upregulated between E8.5 and E9.5 in the hindbrain in r5; coincidentally from E8.5 the posterior expression domain of *Hoxb1* is down-regulated and later turned off in r5 and posterior hindbrain and established a sharp

r4/r5 boundary (data shown in Fig. 3). Therefore, *Hoxb3* represses *Hoxb1* expression in the caudal hindbrain from E8.5 to E10.5 to maintain the spatial colinearity of *Hox* expression during hindbrain patterning, such that *Hoxb1* expression is restricted to r4 to determine the appropriate neurogenesis process for this rhombomere.

The normal establishment of *Hoxb1* expression domain is subjected to a complex network of cross- and auto-regulation among different *Hox* members (Gavalas et al., 2003; Gavalas et al., 1998; Gavalas et al., 2001; Murphy and Hill, 1991; Rossel and Capecchi, 1999; Studer et al., 1998) as well as other transcriptional regulators (Barrow et al., 2000; Ferretti et al., 2005; Popperl et al., 1995). As summarized in Fig. 7B,C, during early development, retinoic acid signaling is required to activate and initiate *Hoxb1* expression through the retinoic acid response element RARE 3'DR2 (Dupe et al., 1997; Huang et al., 2002; Marshall et al., 1994). *Hoxb1* expression in r4 is then maintained by *Hoxb1* as well as *Hoxa1* through an auto-regulatory element B1ARE located at the 5'flanking region of the *Hoxb1* gene (Gavalas et al., 1998; Gavalas et al., 2001; Popperl et al., 1995; Studer et al., 1998). By E9.5, a second negative regulation is triggered by retinoic acid signaling through a separate RARE element 5'DR2 to repress the expression of *Hoxb1* in r3 and r5 (Marshall et al., 1996; Studer et al., 1994). It has been proposed that additional elements are needed as the r3/r5 repressor is insufficient to restrict *Hoxb1* expression in r4 (Fox, 2000). In this study, we identified a Hoxb3 binding site S3 which is located at the 3' flanking region of *Hoxb1* gene (Fig. 7B). By a series of in vivo ChIP analysis, we have shown that in both P19 cells and in mouse embryos, endogenously expressed Hoxb3 was consistently bound to the S3 site of the *Hoxb1* gene. Using

chromatin extracted from caudal hindbrain and anterior spinal cord tissue of E9.5 wildtype mouse embryos, we could clearly detect direct binding of Hoxb3 to the S3 site of *Hoxb1*. We have further demonstrated that the S3 site was a functional repressor site; upon Hoxb3 binding to the S3 site, *Hoxb1* directed gene expression was repressed as shown in chick in ovo electroporation experiments. Our results shown here have provided the molecular mechanism for the function of *Hoxb3* as a direct negative regulator of *Hoxb1*.

The role of *Hoxb3* as a negative regulator of *Hoxb1* is further supported by loss-of-function mutant studies. In *Hox3* loss-of-function mutants, *Hoxb1* expression was de-repressed in r6, with associated activation of r4-like FBMs differentiation and migration in r6 (Gaufo et al., 2003). Therefore, while *Hoxa3*, *Hoxb3* and *Hoxd3* share functional redundancy, there is strong genetic evidence that they are required to suppress *Hoxb1* expression in r6 to prevent it from adopting a r4-like identity.

In addition to cross-regulation by other *Hox* genes, other regulations are also in place to restrict the expression of *Hoxb1* to r4 in the hindbrain. *Krox20* is another negative regulator, by interacting with PIASxβ it represses *Hoxb1* expression in r3 and r5 (Garcia-Dominguez et al., 2006; Giudicelli et al., 2001). Therefore, *Hoxb3*, *Krox20* and retinoic acid signaling are all involved in the suppression of *Hoxb1* in the hindbrain to restrict *Hoxb1* expression to r4. In particular, the suppression of *Hoxb1* in r5 and the posterior hindbrain by *Hoxb3* is initiated from E8.5, hence *Hoxb3* acts earlier than the RARE 5'DR2 r3/r5 repressor. In conclusion, *Hoxb3* is an important negative regulator for

both temporal and spatial restriction of *Hoxb1* expression in r4 in mouse hindbrain patterning.

Acknowledgements

We thank Dr. Nancy Manley for the *Hoxb3*$^{-/-}$ knockout mice; Ms. S.L. Tsang, Dr. Keith Leung and the Transgenic Core Facility for technical support and animal husbandry; Drs. Martin Cheung and L.A. Osorio Da Silva for assistance in chick in ovo electroporation experiments. This work was supported by research grants from the Hong Kong Research Grants Council (HKU7294/98M, HKU2/01C, HKU4/05C, HKU775209M).

Reference

Arenkiel, B. R., Tvrdik, P., Gaufo, G. O., Capecchi, M. R., 2004. Hoxb1 functions in both motoneurons and in tissues of the periphery to establish and maintain the proper neuronal circuitry. Genes Dev. 18**,** 1539-52.

Barrow, J. R., Stadler, H. S., Capecchi, M. R., 2000. Roles of Hoxa1 and Hoxa2 in patterning the early hindbrain of the mouse. Development. 127**,** 933-44.

Bouillet, P., Oulad-Abdelghani, M., Ward, S.J., Bronner, S., Chambon, P., Dolle, P. 1996. A new mouse member of the Wnt gene family, mWnt-8, is expressed during early embryogenesis and is ectopically induced by retinoic acid. Mech. Dev. 58, 141-52.

Briscoe, J., Wilkinson, D. G., 2004. Establishing neuronal circuitry: Hox genes make the connection. Genes Dev. 18**,** 1643-8.

Carpenter, E. M., Goddard, J. M., Chisaka, O., Manley, N. R., Capecchi, M. R., 1993. Loss of Hox-A1 (Hox-1.6) function results in the reorganization of the murine hindbrain. Development. 118**,** 1063-75.

Dessaud, E., Yang, L. L., Hill, K., Cox, B., Ulloa, F., Ribeiro, A., Mynett, A., Novitch, B. G., Briscoe, J., 2007. Interpretation of the sonic hedgehog morphogen gradient by a temporal adaptation mechanism. Nature. 450**,** 717-20.

Duboule, D., Morata, G., 1994. Colinearity and functional hierarchy among genes of the homeotic complexes. Trends Genet. 10**,** 358-64.

Dupe, V., Davenne, M., Brocard, J., Dolle, P., Mark, M., Dierich, A., Chambon, P., Rijli, F. M., 1997. In vivo functional analysis of the Hoxa-1 3' retinoic acid response element (3'RARE). Development. 124**,** 399-410.

Ferretti, E., Cambronero, F., Tumpel, S., Longobardi, E., Wiedemann, L. M., Blasi, F., Krumlauf, R., 2005. Hoxb1 enhancer and control of rhombomere 4 expression: complex interplay between PREP1-PBX1-HOXB1 binding sites. Mol Cell Biol. 25**,** 8541-52.

Ferretti, E., Marshall, H., Popperl, H., Maconochie, M., Krumlauf, R., Blasi, F., 2000. Segmental expression of Hoxb2 in r4 requires two separate sites that integrate cooperative interactions between Prep1, Pbx and Hox proteins. Development. 127**,** 155-66.

Fox, E. A., 2000. The previously identified r3/r5 repressor may require the cooperation of additional negative elements for rhombomere restriction of Hoxb1. Brain Res Dev Brain Res. 120**,** 151-64.

Fraser, S., Keynes, R., Lumsden, A., 1990. Segmentation in the chick embryo hindbrain is defined by cell lineage restrictions. Nature. 344**,** 431-5.

Fritzsch, B., Nichols, D. H., 1993. DiI reveals a prenatal arrival of efferents at the differentiating otocyst of mice. Hear Res. 65**,** 51-60.

Garcia-Dominguez, M., Gilardi-Hebenstreit, P., Charnay, P., 2006. PIASxbeta acts as an activator of Hoxb1 and is antagonized by Krox20 during hindbrain segmentation. Embo J. 25**,** 2432-42.

Gaufo, G. O., Flodby, P., Capecchi, M. R., 2000. Hoxb1 controls effectors of sonic hedgehog and Mash1 signaling pathways. Development. 127**,** 5343-54.

Gaufo, G. O., Thomas, K. R., Capecchi, M. R., 2003. Hox3 genes coordinate mechanisms of genetic suppression and activation in the generation of branchial and somatic motoneurons. Development. 130**,** 5191-201.

Gavalas, A., Ruhrberg, C., Livet, J., Henderson, C. E., Krumlauf, R., 2003. Neuronal defects in the hindbrain of Hoxa1, Hoxb1 and Hoxb2 mutants reflect regulatory interactions among these Hox genes. Development. 130**,** 5663-79.

Gavalas, A., Studer, M., Lumsden, A., Rijli, F. M., Krumlauf, R., Chambon, P., 1998. Hoxa1 and Hoxb1 synergize in patterning the hindbrain, cranial nerves and second pharyngeal arch. Development. 125**,** 1123-36.

Gavalas, A., Trainor, P., Ariza-McNaughton, L., Krumlauf, R., 2001. Synergy between Hoxa1 and Hoxb1: the relationship between arch patterning and the generation of cranial neural crest. Development. 128**,** 3017-27.

Giudicelli, F., Taillebourg, E., Charnay, P., Gilardi-Hebenstreit, P., 2001. Krox-20 patterns the hindbrain through both cell-autonomous and non cell-autonomous mechanisms. Genes Dev. 15**,** 567-80.

Goddard, J. M., Rossel, M., Manley, N. R., Capecchi, M. R., 1996. Mice with targeted disruption of Hoxb-1 fail to form the motor nucleus of the VIIth nerve. Development. 122**,** 3217-28.

Guidato, S., Prin, F., Guthrie, S., 2003. Somatic motoneurone specification in the hindbrain: the influence of somite-derived signals, retinoic acid and Hoxa3. Development. 130**,** 2981-96.

Hu, M. C., Rosenblum, N. D., 2005. Smad1, beta-catenin and Tcf4 associate in a molecular complex with the Myc promoter in dysplastic renal tissue and cooperate to control Myc transcription. Development. 132**,** 215-25.

Huang, D., Chen, S. W., Gudas, L. J., 2002. Analysis of two distinct retinoic acid response elements in the homeobox gene Hoxb1 in transgenic mice. Dev Dyn. 223**,** 353-70.

Jacob, J., Ferri, A. L., Milton, C., Prin, F., Pla, P., Lin, W., Gavalas, A., Ang, S. L., Briscoe, J., 2007. Transcriptional repression coordinates the temporal switch from motor to serotonergic neurogenesis. Nat Neurosci. 10**,** 1433-9.

Keynes, R., Krumlauf, R., 1994. Hox genes and regionalization of the nervous system. Annu Rev Neurosci. 17**,** 109-32.

Kulesa, P. M., Fraser, S. E., 1998. Segmentation of the vertebrate hindbrain: a time-lapse analysis. Int J Dev Biol. 42**,** 385-92.

Kulesa, P. M., Fraser, S. E., 2000. In ovo time-lapse analysis of chick hindbrain neural crest cell migration shows cell interactions during migration to the branchial arches. Development. 127**,** 1161-72.

Lumsden, A., Krumlauf, R., 1996. Patterning the vertebrate neuraxis. Science. 274**,** 1109-15.

Maconochie, M., Nonchev, S., Morrison, A., Krumlauf, R., 1996. Paralogous Hox genes: function and regulation. Annu Rev Genet. 30**,** 529-56.

Maconochie, M. K., Nonchev, S., Studer, M., Chan, S. K., Popperl, H., Sham, M. H., Mann, R. S., Krumlauf, R., 1997. Cross-regulation in the mouse HoxB complex: the expression of Hoxb2 in rhombomere 4 is regulated by Hoxb1. Genes Dev. 11**,** 1885-95.

Manley, N. R., Capecchi, M. R., 1997. Hox group 3 paralogous genes act synergistically in the formation of somitic and neural crest-derived structures. Dev Biol. 192**,** 274-88.

Manzanares, M., Cordes, S., Ariza-McNaughton, L., Sadl, V., Maruthainar, K., Barsh, G., Krumlauf, R., 1999. Conserved and distinct roles of kreisler in regulation of the paralogous Hoxa3 and Hoxb3 genes. Development. 126**,** 759-69.

Marshall, H., Morrison, A., Studer, M., Popperl, H., Krumlauf, R., 1996. Retinoids and Hox genes. Faseb J. 10**,** 969-78.

Marshall, H., Studer, M., Popperl, H., Aparicio, S., Kuroiwa, A., Brenner, S., Krumlauf, R., 1994. A conserved retinoic acid response element required for early expression of the homeobox gene Hoxb-1. Nature. 370**,** 567-71.

Morata, G., 1993. Homeotic genes of Drosophila. Curr Opin Genet Dev. 3**,** 606-14.

Murphy, P., Hill, R. E., 1991. Expression of the mouse labial-like homeobox-containing genes, Hox 2.9 and Hox 1.6, during segmentation of the hindbrain. Development. 111**,** 61-74.

Okada, Y., Shimazaki, T., Sobue, G., Okano, H., 2004. Retinoic-acid-concentration-dependent acquisition of neural cell identity during in vitro differentiation of mouse embryonic stem cells. Dev Biol. 275**,** 124-42.

Pata, I., Studer, M., van Doorninck, J. H., Briscoe, J., Kuuse, S., Engel, J. D., Grosveld, F., Karis, A., 1999. The transcription factor GATA3 is a downstream effector of Hoxb1 specification in rhombomere 4. Development. 126**,** 5523-31.

Pattyn, A., Vallstedt, A., Dias, J. M., Samad, O. A., Krumlauf, R., Rijli, F. M., Brunet, J. F., Ericson, J., 2003. Coordinated temporal and spatial control of motor neuron and serotonergic neuron generation from a common pool of CNS progenitors. Genes Dev. 17**,** 729-37.

Popperl, H., Bienz, M., Studer, M., Chan, S. K., Aparicio, S., Brenner, S., Mann, R. S., Krumlauf, R., 1995. Segmental expression of Hoxb-1 is controlled by a highly conserved autoregulatory loop dependent upon exd/pbx. Cell. 81**,** 1031-42.

Rossel, M., Capecchi, M. R., 1999. Mice mutant for both Hoxa1 and Hoxb1 show extensive remodeling of the hindbrain and defects in craniofacial development. Development. 126**,** 5027-40.

Sham, M. H., Hunt, P., Nonchev, S., Papalopulu, N., Graham, A., Boncinelli, E., Krumlauf, R., 1992. Analysis of the murine Hox-2.7 gene: conserved alternative transcripts with differential distributions in the nervous system and the potential for shared regulatory regions 35. EMBO J. 11**,** 1825-1836.

Studer, M., Gavalas, A., Marshall, H., Ariza-McNaughton, L., Rijli, F. M., Chambon, P., Krumlauf, R., 1998. Genetic interactions between Hoxa1 and Hoxb1 reveal new roles in regulation of early hindbrain patterning. Development. 125**,** 1025-36.

Studer, M., Lumsden, A., Ariza-McNaughton, L., Bradley, A., Krumlauf, R., 1996. Altered segmental identity and abnormal migration of motor neurons in mice lacking Hoxb-1. Nature. 384**,** 630-4.

Studer, M., Popperl, H., Marshall, H., Kuroiwa, A., Krumlauf, R., 1994. Role of a conserved retinoic acid response element in rhombomere restriction of Hoxb-1. Science. 265**,** 1728-32.

Tumpel, S., Wiedemann, L. M., Krumlauf, R., 2009. Hox genes and segmentation of the vertebrate hindbrain. Curr Top Dev Biol. 88**,** 103-37.

Wilkinson, R., Kotlarski, I., Barton, M., Phillips, P., 1992. Isolation of koala lymphoid cells and their in vitro responses to mitogens. Vet.Immunol.Immunopathol. 31**,** 21-33.

Yau, T. O., Kwan, C. T., Jakt, L. M., Stallwood, N., Cordes, S., Sham, M. H., 2002. Auto/cross-regulation of Hoxb3 expression in posterior hindbrain and spinal cord. Dev Biol. 252**,** 287-300.

Table 1. The penetrant rate for gross and behavioural abnormalities of *Hoxb3*^{Tg} gain-of-function transgenic mutant mice

Phenotype	% of transgenic mutants affected			
	*Transgenic founders (n=8)	*Hoxb3*^{Tg2} offspring (n=30)	*Hoxb3*^{Tg7} offspring (n=30)	*Hoxb3*^{Tg8} offspring (n=30)
Reduced pinna size				
• Bilateral reduction	75	80	10	30
• Unilateral reduction	0	10	0	20
• No reduction	25	10	90	50
Impaired whisker movement				
• Bilateral impairment	62.5	60	30	50
• Unilateral impairment	0	30	10	30
• No impairment	37.5	10	60	20
Facial paralysis	62.5	90	40	80
Head tilting response	75	100	100	100
Circling response	62.5	100	100	100
Abnormal reaching response	75	100	100	100
Abnormal preyer reflex	75	100	100	100

*The 8 independent transgenic founders *Hoxb3-Tg1* to -*Tg8*

Figure Legends

Figure 1. Generation of *Hoxb3*^{Tg} mutant mice. (A) Diagram showing transgenic DNA construct with *Hoxb2* r4 enhancer and *Hoxb3* coding region. Triangle: *Prep/Meis* binding site; oval: *Hoxb1/Pbx* binding site; arrowheads: positions of primers for PCR genotyping *Hoxb3*^{Tg} mutants which generate a 450 bp band as shown. (B) Southern blot analysis of *Sac*I cut genomic DNA from *Hoxb3-Tg2, Tg7* and *Tg8* mouse lines using *Bgl*II-*Eco*RI *Hoxb2* fragment as probe. The 11.5 kb band is the endogenous *Hoxb2* genomic fragment (WT); 5 kb band is from tandem repeats of the *Hoxb3* transgenic construct (Tg); other bands are derived from transgene integration sites. (C) Western blot analysis of Hoxb3 protein expression in the ectopic sites r4/2nd BA in E10.5 wildtype, *Hoxb3*$^{Tg2/+}$, *Hoxb3*$^{Tg7/+}$ and *Hoxb3*$^{Tg8/+}$ transgenic embryos. (D) Whole-mount *in situ* hybridization analysis of *Hoxb3* expression in WT and *Hoxb3*$^{Tg/+}$ embryos at E9.0-E10.5. Arrowheads in *Hoxb3*$^{Tg/+}$ mark the ectopic sites of *Hoxb3* expression; numbers indicate branchial arch.

Figure 2. Craniofacial abnormalities in *Hoxb3*$^{Tg2/+}$ mutants. *Hoxb3*$^{Tg2/+}$ mutant mice have a narrower face (E), receded lower lip (F) and abnormal reaching response (G) compared with wildtype (A-C). Examination of the facial nerve at adult stage showed the absence of the mandibular branch of the facial nerve in *Hoxb3*$^{Tg2/+}$ mutants (H, asterisk). zb, zygomatic branch; bb, buccal branch; mb, mandibular branch.

Figure 3. *Hoxb1* expression is abolished in r4 of *Hoxb3*$^{Tg/+}$ embryos. Wildtype and *Hoxb3*$^{Tg/+}$ mutant embryos (E7.5-10.5) were examined by whole-mount *in situ*

hybridization using *Hoxb3* (A-H), *Hoxb1* (I-L, N-Q), *Hoxb2* (M,R), *Wnt8a* (S,U), *Kr* (T,V), *Krox20* (W,Y) and *EphA4* (X,Z) riboprobes. Arrowheads indicate r5 (F) and r4 (J); asterisks indicate ectopic r4.

Figure 4. Abnormal neurogenesis in r4 of *Hoxb3*$^{Tg/+}$ mutant E11.5 embryos. (A-J) Flat-mounted embryos analysed by whole-mount *in situ* hybridization using *Islet1* (A,F), *Phox2b* (B,G), *Tbx20* (C,H), *Gata3* (D,I) and *Gata2* (E,J) riboprobes. Neuronal tract tracing of FBM (K, M) and CVA (L,N) neurons in wildtype and *Hoxb3*$^{Tg/+}$ mutant hindbrains. Immunostaining of neuronal subtypes using Islet1 (O,P), 5-HT (Q,R) and Lim3 (S,T) antibodies on transverse sections through r2, r4 and r6 of wildtype and *Hoxb3*$^{Tg/+}$ mutant hindbrains. The abnormal generation of ectopic 5-HT^{+} serotonergic neurons (Blue), reduced Islet1^{+} motor neurons (Green) associated with the ventral shift of Lim3^{+} (Red) interneurons are summarized in the schematic diagram. Asterisks indicate abnormal neurogenesis in r4. SN, serotonergic neurons; MN, motor nucleus; V2, interneurons.

Figure 5. Identification of Hoxb3 binding sites in the *Hoxb1* gene locus. (A) Alignment of *Hoxb1* 5' and 3' flanking region sequences from mouse, rat, human, orangutan, dog and cow. Three potential Hoxb3 binding sites S1-S3 were found in the conserved region. (B) Comparison of the sequences of the S1, S2 and S3 binding sites and the Hoxb3 consensus binding site, with the core sequence underlined. (C) Electrophoretic Mobility Shift Assay of Hoxb3 protein and the S3 site on *Hoxb1*. Hoxb3-GST fusion protein can bind to oligonucleotide containing wildtype S3 sequence. The amount of protein,

wildtype and mutant oligonucleotides used are as indicated, the sequences of the mutant oligonucleotides (S3-M1, M2, M12) are as shown.

Figure 6. Hoxb3 protein can bind to the S3 site on *Hoxb1* and suppress *Hoxb1* gene expression *in vivo*. (A) Chromatin immunoprecipitation (ChIP) analysis using RA-treated P19 cell nuclear extracts. Primers were designed to amplify chromatin fragments which contain S1, B1ARE/S2, S3 and B3ARE sites. Hoxb3 could bind to the S3 site on *Hoxb1*, but not S1 nor S2 sites. As positive control we showed that Hoxb3 can bind to the B3ARE site on the *Hoxb3* gene; as negative control we showed that neither Hoxb1 nor Hoxb4 can bind to the S3 site, though Hoxb1 can bind to the B1ARE site. (B) In vivo ChIP analysis using chromatin extracts from forebrain (1), r4/2nd BA (2), caudal hindbrain/spinal cord (3) of E9.5 wildtype, *Hoxb3*^{Tg} and *Hoxb3*$^{-/-}$ null mutant embryos. In wildtype embryos, Hoxb3 protein could bind to the S3 and B3ARE sites in the caudal hindbrain/spinal cord (3). In *Hoxb3*$^{Tg/+}$ mutant embryos. Hoxb3 could bind to the S3 and B3ARE sites in extracts of r4/2nd BA (2) and caudal hindbrain/spinal cord (3). No binding could be detected in extracts from *Hoxb3*$^{-/-}$ mutant embryos. (C) Chick *in ovo* luciferase activity assay with Hoxb3 expression vector and Hoxb1 luciferase reporter. Co-electroporation of Hoxb3 expression vector and wildtype Hoxb1-luc showed that Hoxb3 expression repressed *Hoxb1* transcriptional activity. The transcriptional repression activity of Hoxb3 is S3 site dependent. Bracket indicates statistical significant difference, n=10.

Figure 7. Hoxb3 is a negative regulator for restricting *Hoxb1* expression domain to r4 in the hindbrain. (A) The complementary expression domains of *Hoxb1* (green) and *Hoxb3* (purple) from E7.5 to 10.5 are dynamically regulated. By genetics and molecular analyses we have shown that *Hoxb3* can repress *Hoxb1* expression and contribute to the restriction of *Hoxb1* expression to r4. (B) Positive and negative regulatory sites for establishment and maintenance of *Hoxb1* expression in r4. RARE 3'DR2 and B1ARE sites mediate initiation and maintenance of *Hoxb1* expression in r4. RARE 5'DR2 mediates suppression of *Hoxb1* expression in r3/r5. Hoxb3 S3 binding site is required for suppression of *Hoxb1* in caudal hindbrain and spinal cord to restrict *Hoxb1* expression domain in the posterior. (C) Cross-regulatory network of *Hox1, 2* and *3* genes in hindbrain r4, r5 to the posterior hindbrain during initiation and maintenance of rhombomeric boundary of *Hoxb1* expression.

Supplementary Figure 1. (A) Craniofacial dysmorphogenesis in the *Hoxb3* transgenic mouse lines *Hoxb3-Tg2* (D-F), *Tg7* (G-I) and *Tg8* (J-L). (A-K) Craniofacial defects in mutant mice. The *Hoxb3*$^{Tg/+}$ mutant mice had narrower face (D,G,J), facial paralysis, impaired whisker movement (E,H,K) and absence of the mandibular branch of the VII nerve (asterisks in F,I,L). bb, buccal branch; mb, mandibular branch; zb, zygomatic branch. (M) *Hoxb1* expression is abolished in r4 of *Hoxb3*$^{Tg2/+}$, *Hoxb3*$^{Tg7/+}$ and *Hoxb3*$^{Tg8/+}$ embryos at E10.5 by whole mount *in situ* hybridization using *Hoxb1* riboprobe.

Supplementary Figure 2. Analysis of expression of *Hoxb2* (A-D) and *Hoxa2* (E-H) in E9.5 wild-type (A,B,E,F) and $Hoxb3^{Tg}$ (C,D,G,H) embryos by wholemount in situ hybridization. In wild-type embryos, *Hoxb2* (A,B) was expressed from r3 to the posterior neural tube and *Hoxa2* (E,F) expressed from r2 to the posterior neural tube at E9.5. In $Hoxb3^{Tg}$ embryos, expression of *Hoxb2* (A,B) was reduced in r4, but expression of *Hoxa2* was not affected (G,H).

Figure

Click here to download high resolution image

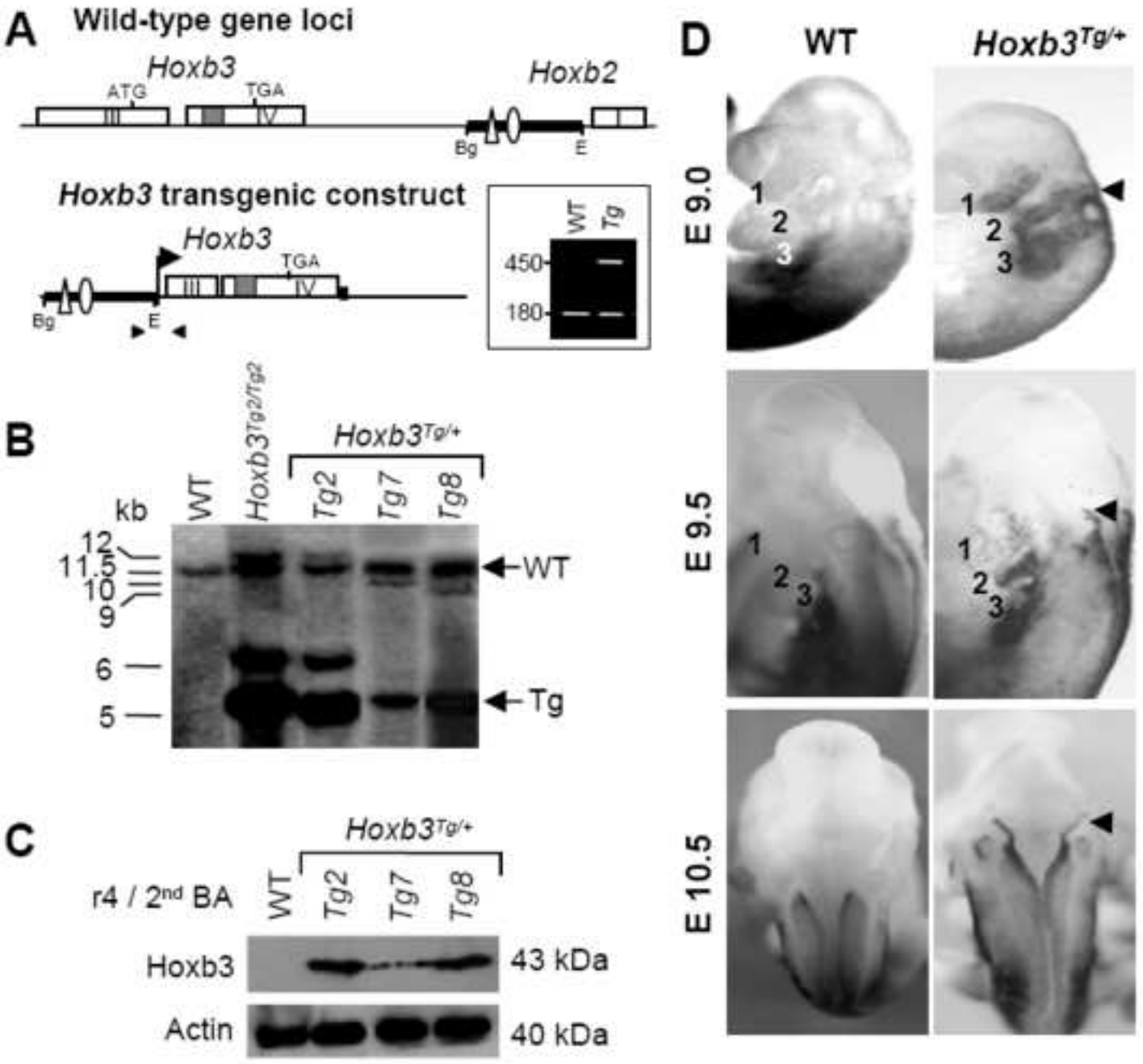

Figure
Click here to download high resolution image

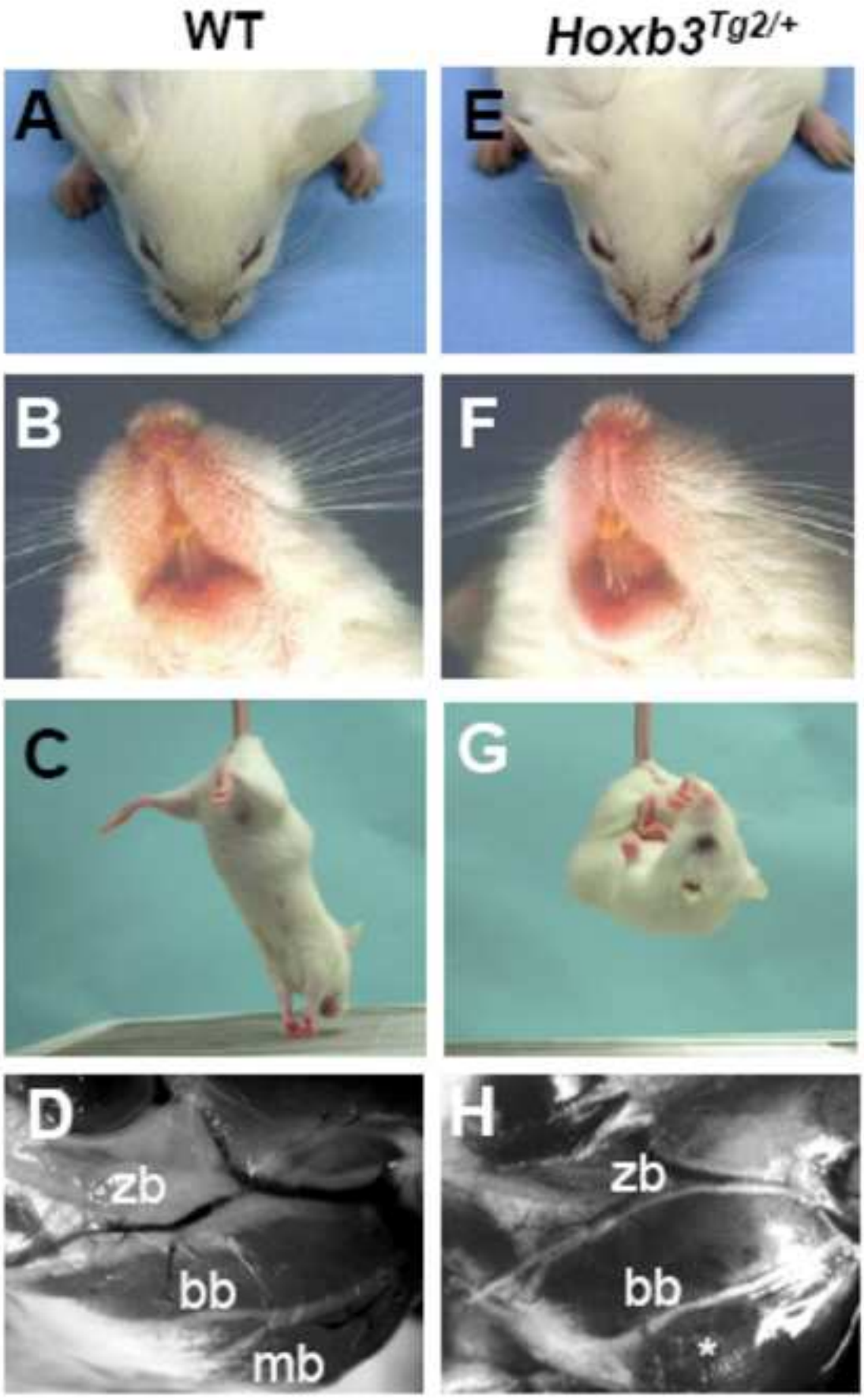

Figure

Click here to download high resolution image

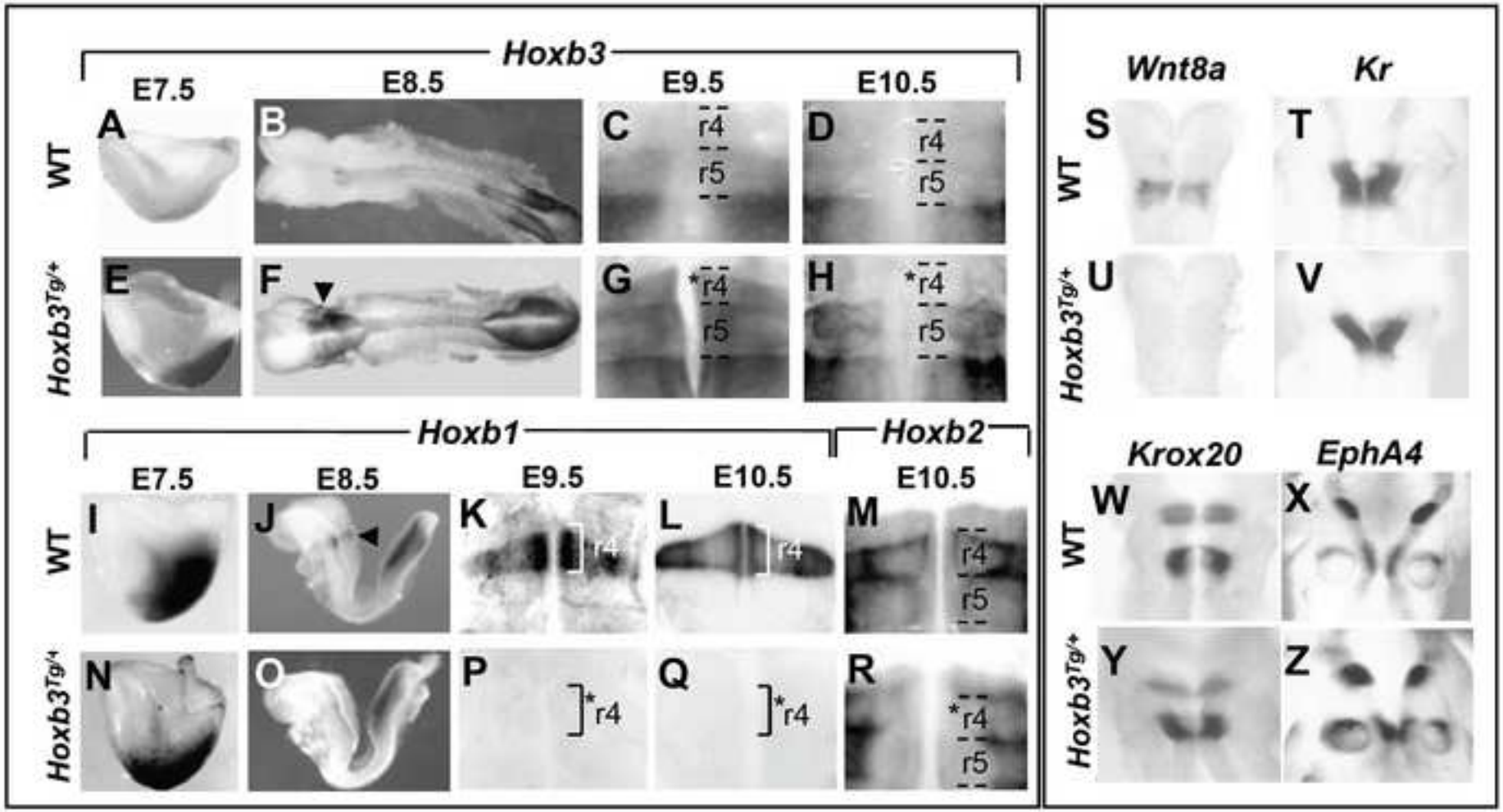

Figure

Click here to download high resolution image

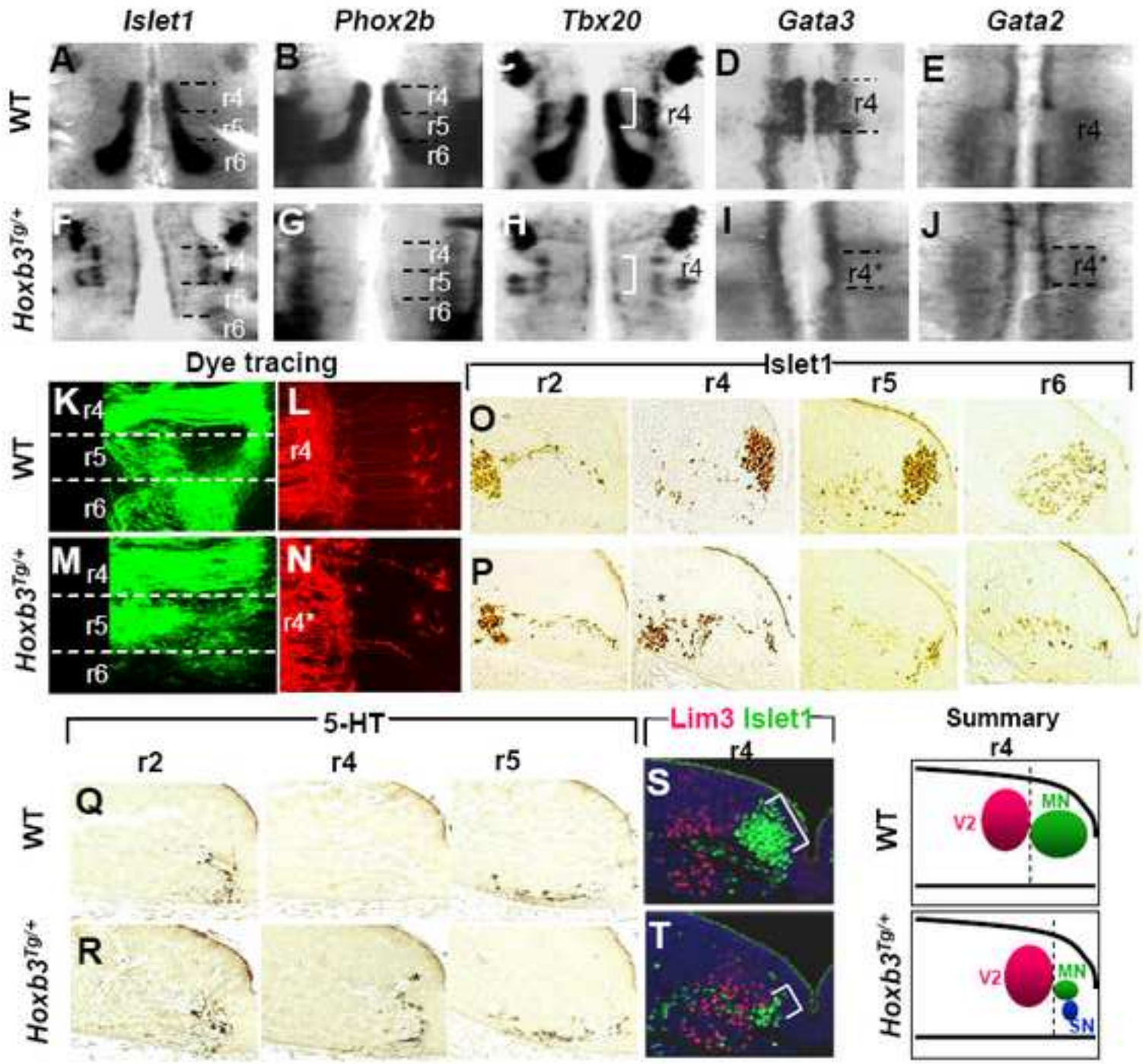

Figure
Click here to download high resolution image

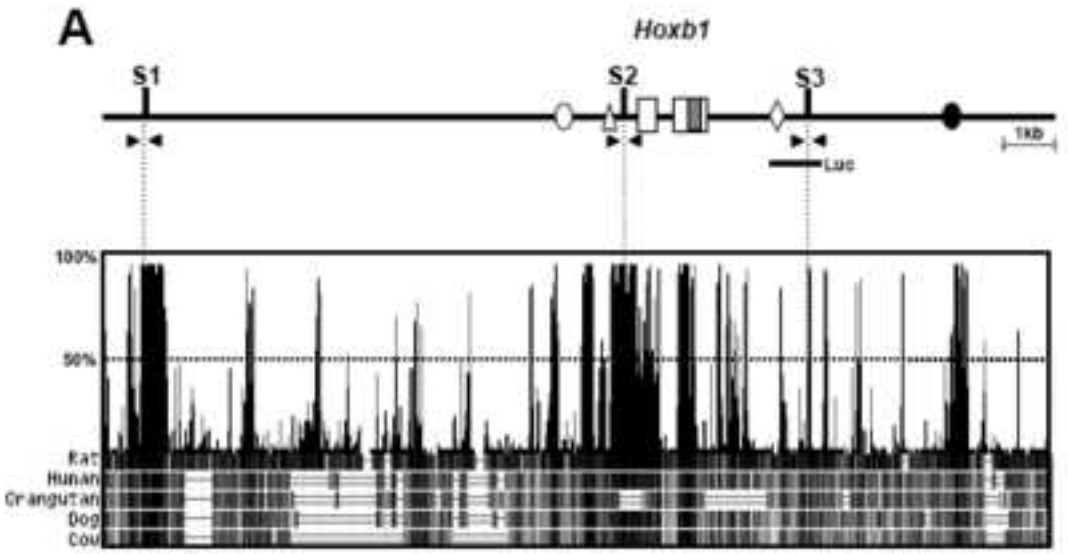

B

Binding sites	Sequence	Sequence similarity to consensus
Consensus	TCATTAATTGGC	
B3ARE	CTTCTAATTATA	83%
S1	ATGAATTAAATA	67%
S2	AATCTAATAATC	67%
S3	CATTTAATTGAA	100%

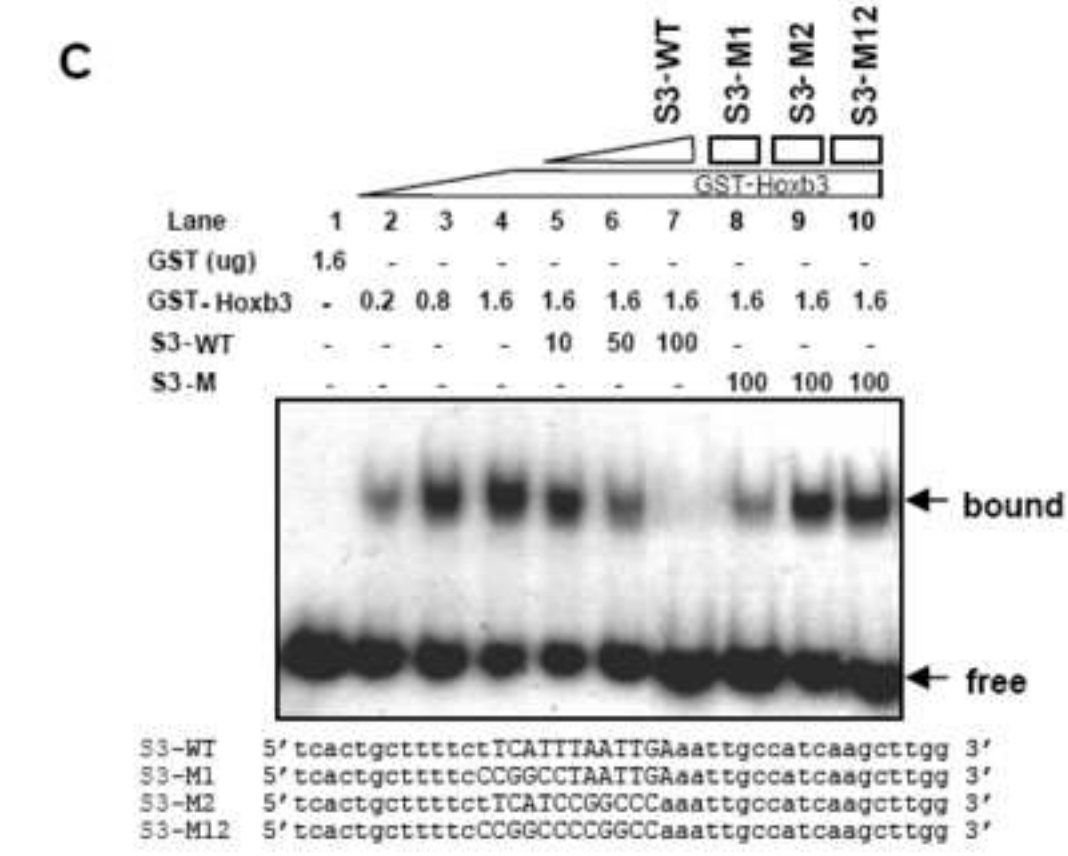

Figure

Click here to download high resolution image

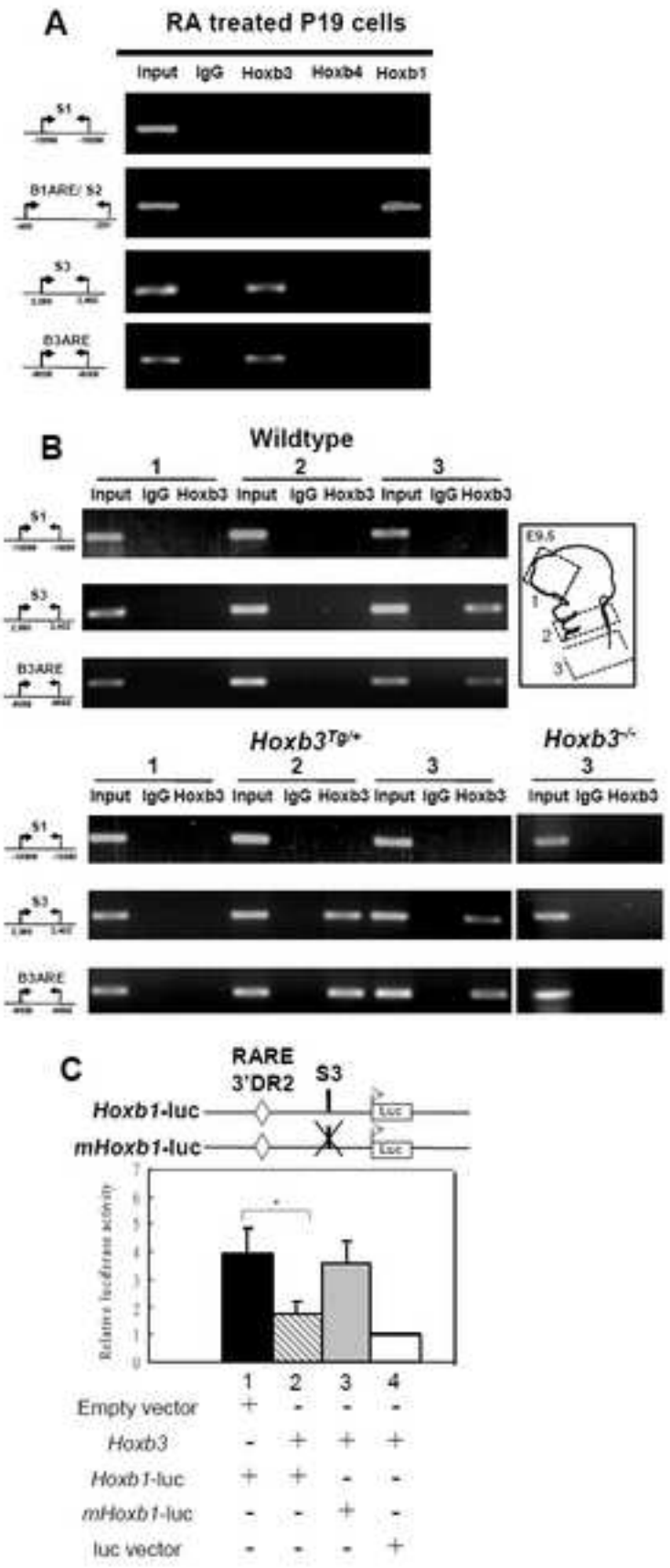

Figure

Click here to download high resolution image

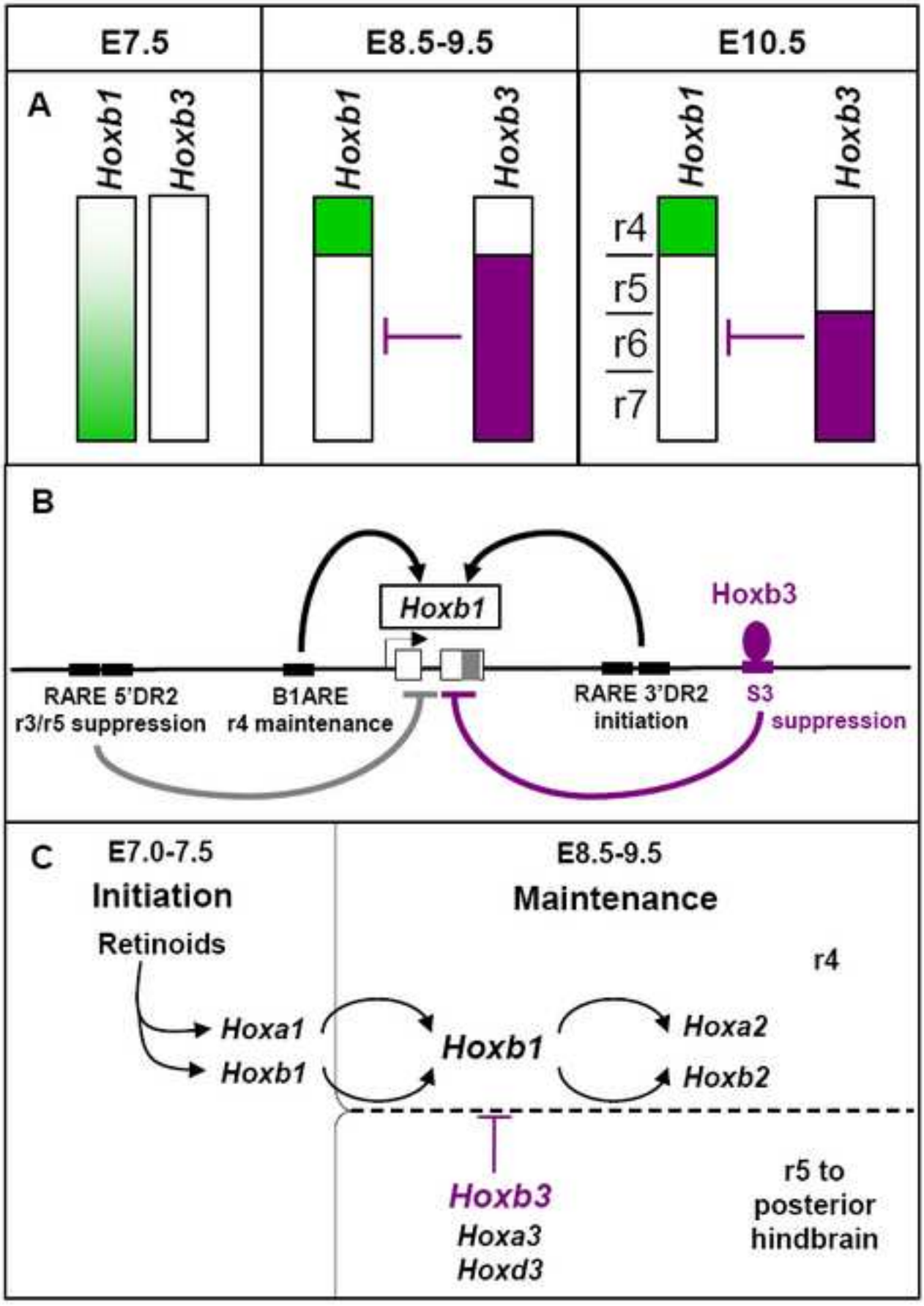

Table 1. The penetrant rate for gross and behavioural abnormalities of *Hoxb3*^{Tg} gain-of-function transgenic mutant mice

Phenotype	% of transgenic mutants affected			
	*Transgenic founders (n=8)	*Hoxb3*^{Tg2} offspring (n=30)	*Hoxb3*^{Tg7} offspring (n=30)	*Hoxb3*^{Tg8} offspring (n=30)
Reduced pinna size				
• Bilateral reduction	75	80	10	30
• Unilateral reduction	0	10	0	20
• No reduction	25	10	90	50
Impaired whisker movement				
• Bilateral impairment	62.5	60	30	50
• Unilateral impairment	0	30	10	30
• No impairment	37.5	10	60	20
Facial paralysis	62.5	90	40	80
Head tilting response	75	100	100	100
Circling response	62.5	100	100	100
Abnormal reaching response	75	100	100	100
Abnormal preyer reflex	75	100	100	100

*The 8 independent transgenic founders *Hoxb3-Tg1* to -*Tg8*

Figure 1

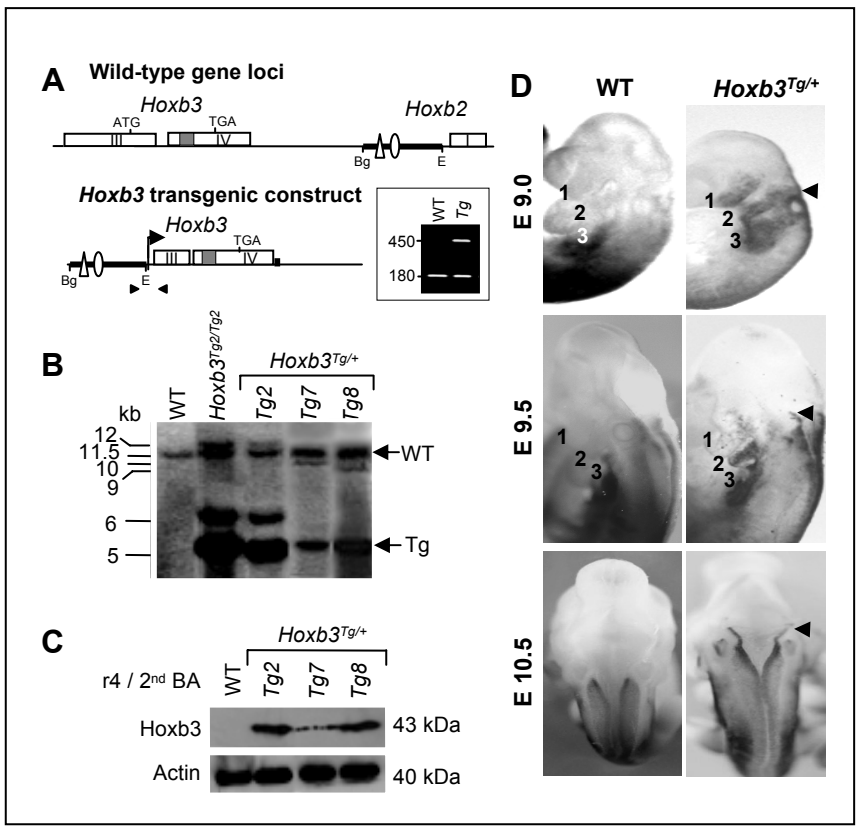
A
Wild-type gene loci
Hoxb3
ATG
TGA
Hoxb2
Bg
E
Hoxb3 transgenic construct
Hoxb3
TGA
Bg
E
WT
Tg
450
180
B
kb
12
11.5
10
9
6
5
WT
Hoxb3Tg2/Tg2
Hoxb3Tg/+
Tg2
Tg7
Tg8
WT
Tg
C
Hoxb3Tg/+
r4 / 2nd BA
WT
Tg2
Tg7
Tg8
Hoxb3
43 kDa
Actin
40 kDa
D
WT
Hoxb3Tg/+
E 9.0
E 9.5
E 10.5
1
2
3

Figure 2

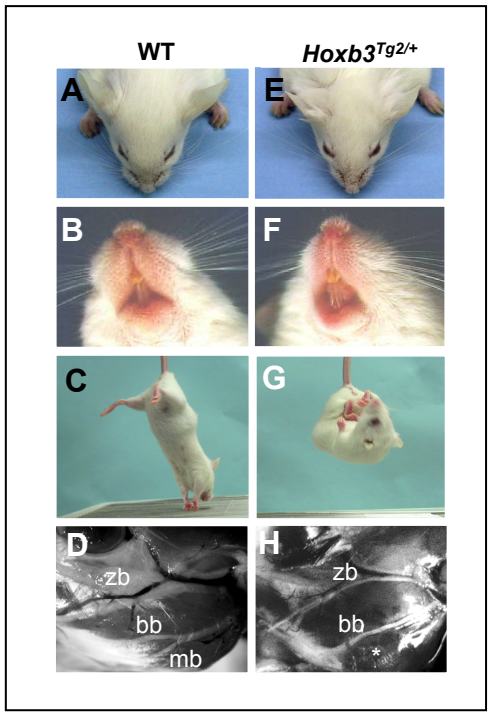

Figure 3

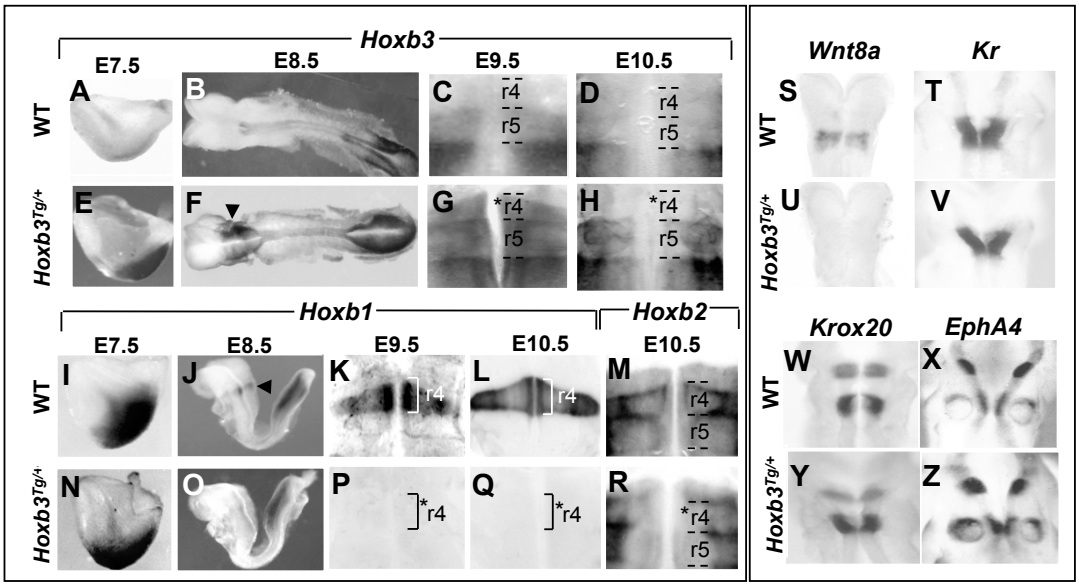
Hoxb3
E7.5
E8.5
E9.5
E10.5
WT
Hoxb3Tg/+
A
B
C
D
E
F
G
H
r4
r5
*r4
Hoxb1
Hoxb2
I
J
K
L
M
N
O
P
Q
R
Wnt8a
Kr
S
T
U
V
Krox20
EphA4
W
X
Y
Z

Figure 4

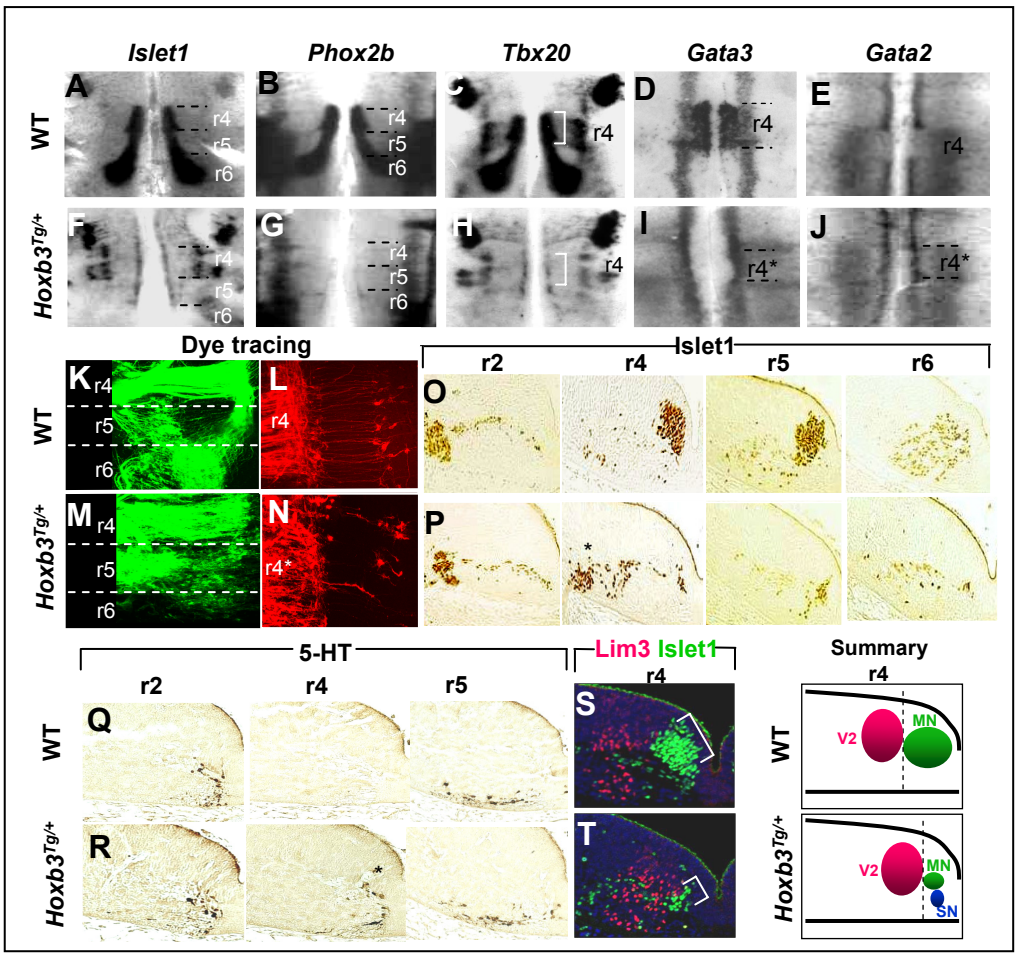
Islet1
Phox2b
Tbx20
Gata3
Gata2
WT
Hoxb3Tg/+
A
B
C
D
E
F
G
H
I
J
r4
r5
r6
r4*
Dye tracing
Islet1
r2
r4
r5
r6
K
L
M
N
O
P
5-HT
Lim3 Islet1
Summary
Q
R
S
T
V2
MN
SN

Figure 5

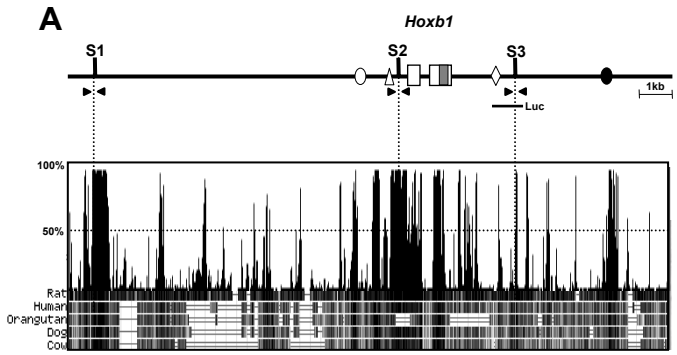

B

Binding sites	Sequence	Sequence similarity to consensus
Consensus	TCATTAATTGGC	
B3ARE	CTTCTAATTATA	83%
S1	ATGAATTAAATA	67%
S2	AATCTAATAATC	67%
S3	CATTTAATTGAA	100%

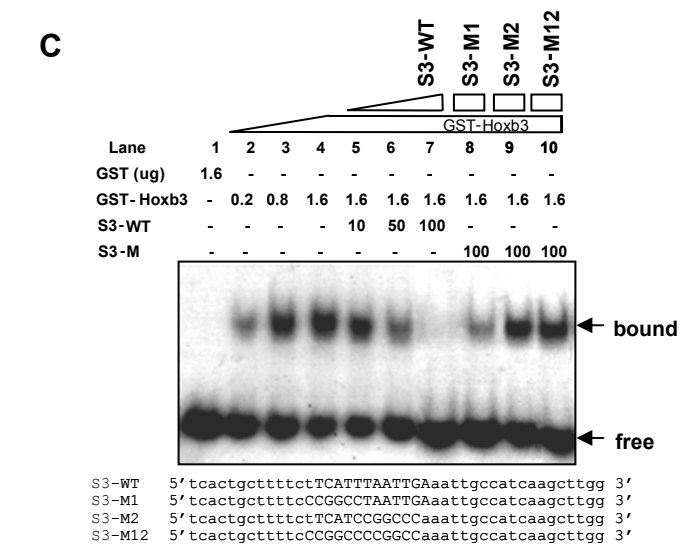

S3-WT 5′tcactgcttttctTCATTTAATTGAaattgccatcaagcttgg 3′
S3-M1 5′tcactgcttttcCCGGCCTAATTGAaattgccatcaagcttgg 3′
S3-M2 5′tcactgcttttctTCATCCGGCCCaaattgccatcaagcttgg 3′
S3-M12 5′tcactgcttttcCCGGCCCCGGCCaaattgccatcaagcttgg 3′

Figure 6

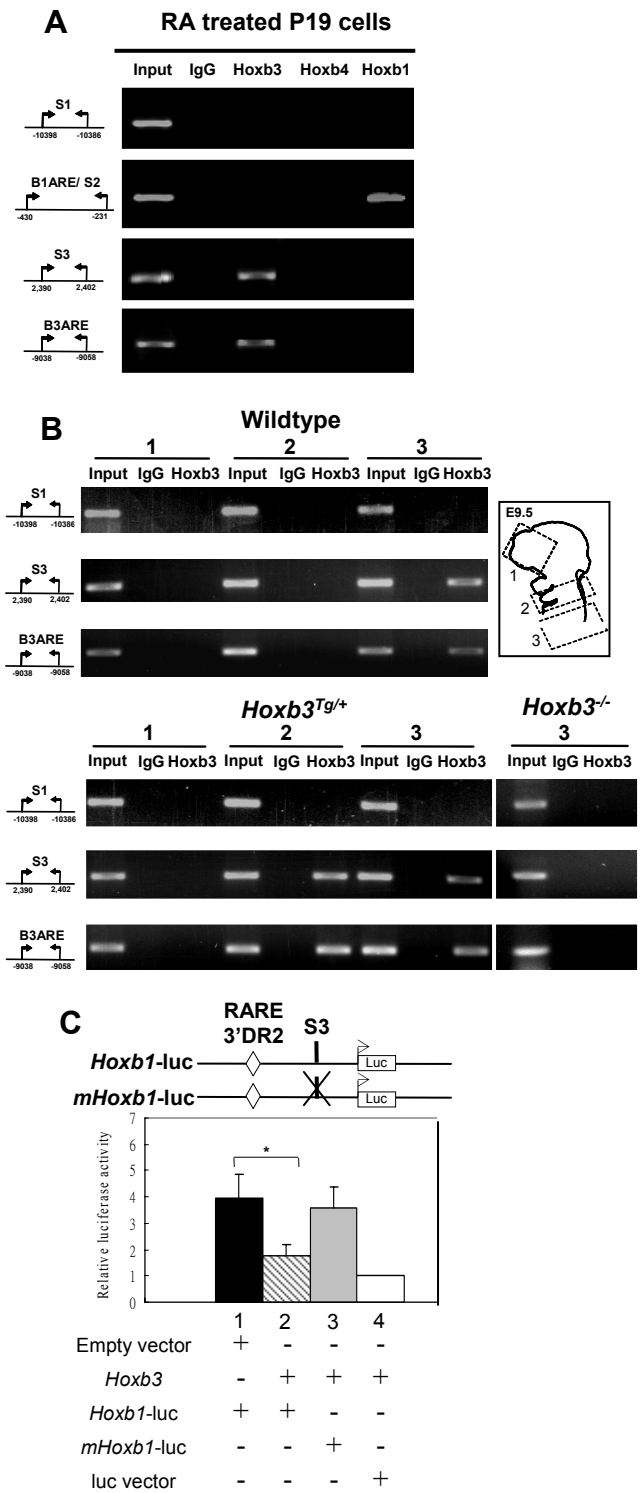
A
RA treated P19 cells
Input IgG Hoxb3 Hoxb4 Hoxb1
S1
-10398 -10386
B1ARE/ S2
-430 -231
S3
2,390 2,402
B3ARE
-9038 -9058
B
Wildtype
1 2 3
Input IgG Hoxb3 Input IgG Hoxb3 Input IgG Hoxb3
E9.5
Hoxb3Tg/+
Hoxb3-/-
C
RARE
3'DR2
S3
Hoxb1-luc
mHoxb1-luc
Luc
Relative luciferase activity
Empty vector
Hoxb3
Hoxb1-luc
mHoxb1-luc
luc vector

Figure 7

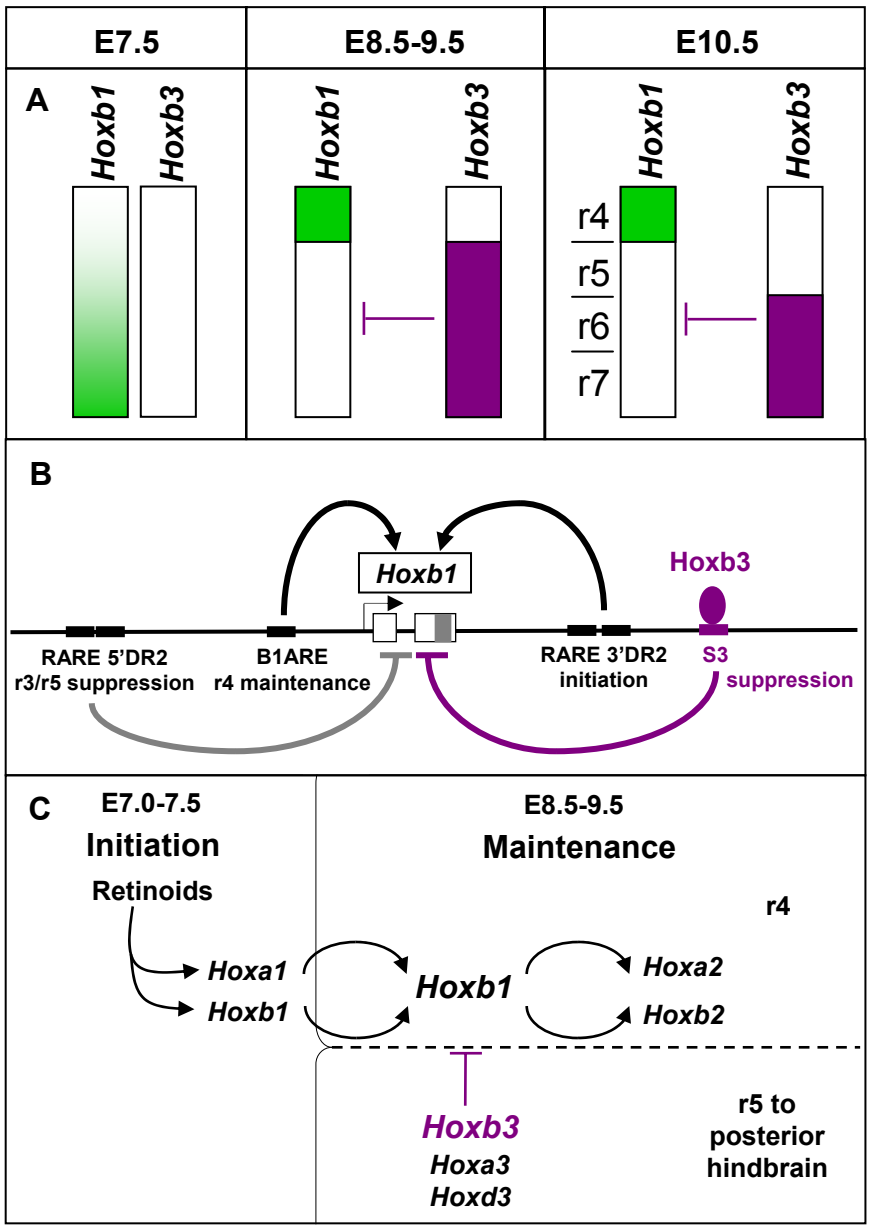
E7.5
E8.5-9.5
E10.5
A
Hoxb1
Hoxb3
r4
r5
r6
r7
B
Hoxb1
Hoxb3
RARE 5'DR2
r3/r5 suppression
B1ARE
r4 maintenance
RARE 3'DR2
initiation
S3
suppression
C
E7.0-7.5
Initiation
Retinoids
Hoxa1
Hoxb1
E8.5-9.5
Maintenance
r4
Hoxb1
Hoxa2
Hoxb2
Hoxb3
Hoxa3
Hoxd3
r5 to
posterior
hindbrain

Supplementary Figure 1

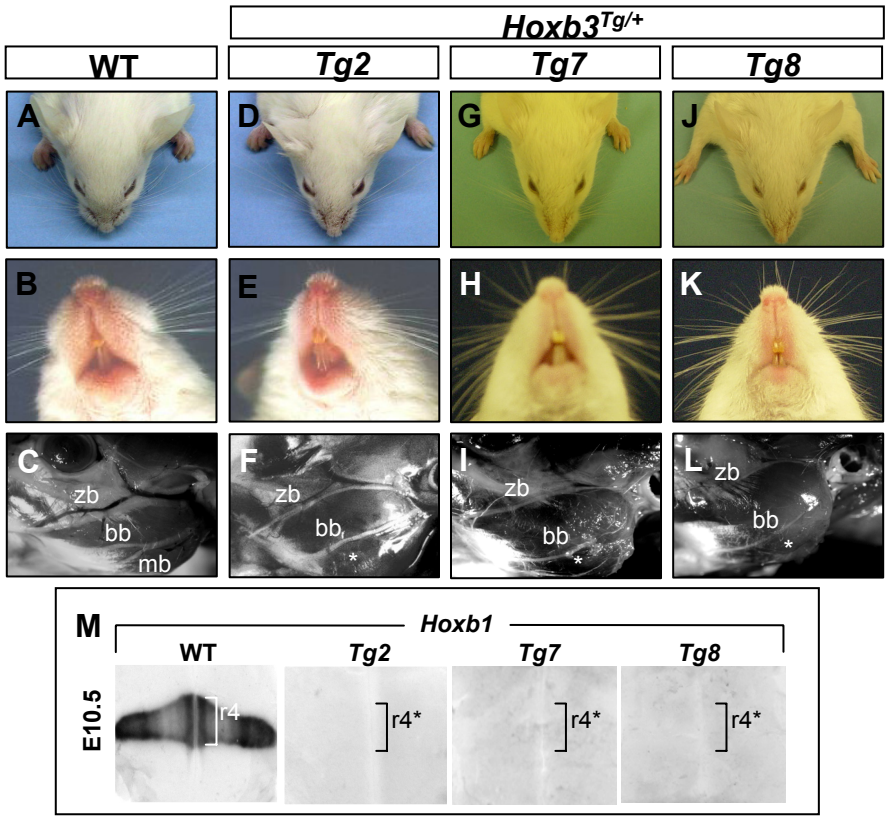

Supplementary Figure 2